Analytic results for wetting transitions in the presence of van der Waals tails

S. Dietrich
Fachbereich Physik, Bergische Universität Wuppertal, Postfach 100127, D-5600 Wuppertal 1, Federal Republic of Germany

M. Napiórkowski
Instytut Fizyki Teoretycznej, Uniwersytet Warszawski, Hoża 69, PL-00-681 Warszawa, Poland
(Received 12 July 1990)

We present a systematic study of the wetting behavior of a one-component fluid at a wall and of interfacial wetting in binary liquid mixtures by taking into account all aspects of the long-range character of the van der Waals interactions between the particles. The corresponding effective interface potential is expressed in terms of those free interfacial profiles that emerge as a consequence of the wetting phenomena. This approach goes beyond previous ones, because we take into account the van der Waals tails of these interfaces, and in the one-component case the structure of the emerging wall-liquid interface. In addition, we discuss the distortion of the actual interface profile—compared with the corresponding free one—caused by a finite thickness of the wetting film. The analytic results allow us to draw conclusions about both the value of the wetting transition temperature for second-order wetting transitions and the size of the critical region for such a transition as well as about the onset of critical adsorption. We also present the exact expressions for the leading van der Waals tails of the liquid-gas, wall-liquid, and wall-gas interfaces in a one-component system as well as for interfaces in binary liquid mixtures. We find that at a critical wetting transition of the wall-gas interfaces, the wall-liquid interface profile undergoes a qualitative structural change.

I. INTRODUCTION

Over a certain range of temperature T and chemical potentials μ_i for various species $i=1,2,\ldots$, a given physical system can exhibit two distinct phases α and γ of condensed matter that are in thermal equilibrium with each other. Such values of μ_i and T allow one to impose boundary conditions such that at $z=-\infty$ the α phase is present and at $z=+\infty$ the γ phase is present. As a consequence, an α-γ interface is formed so that, as described by interfacial profiles, the physical properties of the system vary smoothly between their corresponding bulk values in the α and γ phases. By additional boundary conditions in the parallel direction $\mathbf{r}_\parallel$, or by external fields like, e.g., gravity, we fix the mean position of the α-γ interface to be located at $z=0$, which we call the center of the *free* α-γ interface, i.e., all other possible interfaces or boundaries are macroscopically far away from the center at $z=0$.

Suppose now that for this configuration the chemical potentials μ_i are changed at constant temperature in such a way that for $\mu_i \to \mu_{i,0}(T)$, a third phase β becomes thermodynamically stable at a triple line $\mu_{i,0}(T)$ of three-phase coexistence between α, β, and γ. It may be that above a certain temperature $T=T_w$ this change of chemical potentials causes a phase transition within the interfacial structure such that a β-like film of thickness $l_0(T,\mu_i)$ is formed at $z=0$, which diverges smoothly at $\mu_i=\mu_{i,0}$. As a consequence of this so-called complete wetting transition at $\mu_{i,0}$, the α-γ interface splits—by the intrusion of a macroscopically thick layer of the β phase—into the two free α-β and β-γ interfaces. Below T_w, l_0 remains finite in the limit $\mu_i \to \mu_{i,0}$ and the α-γ interface is not wetted by the β phase. Consequently, along the triple line $\mu_{i,0}(T)$ T_w is the locus of a wetting transition at three-phase coexistence such that $l_0(T) \equiv l_0(T,\mu_{i,0}(T)) < \infty$ for $T < T_w$ and infinite for $T > T_w$. Accordingly above T_w and at three-phase coexistence $\mu_i=\mu_{i,0}$ the three possible surface tensions fulfill Antonov's rule, i.e., $\sigma_{\alpha\gamma}=\sigma_{\alpha\beta}+\sigma_{\beta\gamma}$, whereas for $T<T_w$ one has $\sigma_{\alpha\gamma}<\sigma_{\alpha\beta}+\sigma_{\beta\gamma}$. If at T_w $l_0(T)$ jumps to its infinite value one has a first-order wetting transition; otherwise one has a continuous wetting transition called critical wetting. There have been numerous efforts to detect these interfacial phase transitions experimentally and to understand them on the basis of statistical mechanics. The present status of this rapidly growing and delicate body of research has been reviewed recently.[1–3]

Here we focus on those two physical systems which, for these wetting phenomena, are the most important ones both from a conceptual and a practical point of view. In the first case α is an inert wall and γ is the gas phase of a one-component ($i=1$) fluid, which coexists along the gas-liquid coexistence line $\mu_0(T)$ with the liquid phase β; $\mu_0(T)$ ends at the critical point (T_c,μ_c). The second system is a binary liquid mixture composed of two species A and B corresponding to $i=1$ and 2, respectively. In this case α is the A-rich liquid, β the B-rich liquid, and γ is the vapor. They coexist along a triple line $(T,\mu_{1,0}(T),\mu_{2,0}(T))$ which ends at a critical end point $(T_{\mathrm{CEP}},\mu_{1,0}(T_{\mathrm{CEP}}),\mu_{2,0}(T_{\mathrm{CEP}}))$, where the difference between the α and β phases vanishes. In both systems all

particles interact via long-range forces that decay $\sim|\mathbf{r}-\mathbf{r}'|^{-6}$ for large separations between them. (We ignore retardation effects.) Here we focus on the influence of this long range of the interactions on the aforementioned interfacial structures.

It has turned out that a particularly transparent analysis of these wetting phenomena can be obtained from the knowledge of the so-called effective interface potential $\Omega_s(l)$. This function represents the α-γ surface tension under the restriction that at the interface position a β-like film of thickness l is present. The actual surface tension and the actual thickness l_0 minimize $\Omega_s(l)$: $\sigma_{\alpha\gamma}=\min_l\Omega_s(l)=\Omega_s(l=l_0)$. Since $\Omega_s(l=\infty)=\sigma_{\alpha\beta}+\sigma_{\beta\gamma}$ the characteristic features of critical and complete wetting—for which l_0 diverges smoothly—are determined by the asymptotic behavior of $\Omega_s(l)$ for large l (see Fig. 3.2 in Ref. 1).

Thus the central theoretical problem is to compute the effective interface potential as a function of l, T, and μ_i and as a functional of the atomic interaction potentials. Until now only approximate solutions of this problem were known. In the case of critical and complete wetting the free α-β and β-γ interfaces emerge continuously out of the α-γ interface structure. Thus it is natural to try to parametrize the aforementioned restricted interface profile, which at its center contains a β-like film of thickness l, in terms of these two free interfaces forced to be a distance l apart from each other. The surface free energy of this configuration yields an approximate value for $\Omega_s(l)$.

Thus far, even within this approximation scheme, no exact solution was found. Instead, various further approximations were applied and the following five results were obtained.

(i) The first approach was devoted to the study of critical wetting of a wall on the basis of a continuous Landau-Ginzburg functional that corresponds to particularly short-range forces.[4] There the authors positioned the analytically known free β-γ interface at $z=l$ and truncated it at the wall $z=0$. The α-β interface was treated simply as a step function $\sim\Theta(z)$. Due to resorting to the Landau-Ginzburg theory the resulting $\Omega_s(l)$ no longer contains the explicit information about the microscopic interaction potentials.

(ii) Later on, the wetting of a wall with an exponentially decaying substrate potential by a fluid with also exponentially decaying interatomic forces was studied by a density functional.[5] This approach allows one to follow directly the dependences on the details of atomic forces. Indeed, by applying the same additional approximations as in (i) surprising subtleties have been discovered.

The derivation of these two analytic results (i) and (ii) is based on the knowledge of the explicit analytic form of the free β-γ interface profile. However, in the presence of the experimentally relevant long-range van der Waals interactions this is no longer available. Thus much more severe approximations had to be made in order to still obtain analytic results for this substantially more difficult problem.

(iii) Significant progress could be made by applying the so-called sharp-kink approximation[6,7] to lattice-gas models for the wetting of a wall and to continuous density functionals for both the wetting of a wall by a one-component system as well as by a binary liquid mixture and for interfacial wetting in binary liquid mixtures.[8] In this approach both the free α-β and the β-γ interface profile are replaced by step functions $\sim\Theta(z-d_w)$ and $\sim\Theta(z-l)$, respectively. To a certain extent this approach treats the α-β interface somewhat better than those in (i) and (ii), because in an approximate way it takes into account the fact that near the wall the hard-core repulsion causes the fluid density to vanish at $z\simeq d_w$, which is given by the sum of the radii of the substrate and the fluid particles.

(iv) At first glance the sharp-kink approximation seems to be very crude. Nonetheless, it yields surprisingly reliable predictions even near T_c where the central width ξ of the smooth variation of the β-γ interface diverges. This puzzle has been resolved by applying the improved soft-kink approximation.[9] In this approach the full smooth variation of the free β-γ interface around its center is taken into account within a fixed and finite width ξ given by the bulk correlation length; outside this width the free β-γ interface profile is again replaced by its constant bulk values. It has turned out that the smoothness of the free β-γ interface on this scale ξ is insignificant for the order of the wetting transition and for the transition temperature of critical wetting.[9]

(v) The soft-kink approximation suppresses the smooth variations of the β-γ interface outside its center, which in the case of long-range forces are known as van der Waals tails. Recently the present authors indicated for the wetting of a wall that also this feature of the free β-γ interface can be incorporated analytically into the effective interface potential.[10] Within this approach for $z>d_w$ the restricted interface profile is taken to be the full free β-γ interface profile, including its tails, positioned at $z=l$; for $z\le d_w$, it vanishes abruptly.

In this paper we derive and present these latter results (Sec. II) and we extend them to the case of interfacial wetting in binary liquid mixtures (Sec. III). In addition, we go even two steps further by taking into account also the smooth variation of the α-β interface profile together with its own van der Waals tail on the β side and by taking into account the fact that the restricted interface profile is not simply given by the two free α-β and β-γ interfaces a distance l apart from each other. As a by-product we present the exact expressions for the leading van der Waals tails of the gas-liquid, wall-liquid, and wall-gas interfaces in a one-component system as well as for the interfaces in binary liquid mixtures. In Sec. IV we summarize and discuss the effects of these van der Waals tails on the various wetting phenomena. Certain technical but nonetheless important points are explained in Appendixes A and B.

We pursue these goals by applying a density-functional theory (see Secs. II and III). Although in principle this is an exact formalism,[11] its actual implementation corresponds to a mean-field approximation. Consequently, we discard both those fluctuations, which cause bulk proper-

ties to deviate from their classical behavior near critical points, and capillary waves of the emerging α-β and β-γ interfaces. Whereas in the present context the former fluctuations are only relevant in the case of a close vicinity of T_w and T_c, the capillary waves are excited even at low temperatures. However, in the presence of long-range forces—as they govern the fluid systems considered here—the capillary waves are known to be irrelevant for the thermal singularities of continuous wetting transitions.[12] Furthermore, in real systems gravity suppresses the buildup of capillary waves with arbitrarily long wavelengths which are not captured by a mean-field description. Correspondingly, in the presence of gravity any actual density profile is given by a convolution of the so-called intrinsic density profile with a Gaussian distribution of the mean interface position [see the discussion of Eq. (2.39) in Ref. 9]. In this sense here and in the following we analyze the mean-field approximation of the *intrinsic density profile*. Within mean-field theory and in the presence of long-range forces the calculation of such intrinsic interfacial profiles is restricted to numerical solutions and therefore a transparent full scan of the whole parameter space of the intermolecular interactions is out of reach (see Refs. 1 and 2 and references therein). In this paper, however, we strive for filling this gap and for gaining a maximum of analytic insight into the wetting behavior of fluid systems with long-range forces. (We restrict our analysis to temperatures above the melting point of the wetting phases, i.e., we do not discuss the formation of solid phases.) Thus we conclude that above the triple point T_t and outside the narrow critical region below T_c of the fluid phases our density-functional approach yields reliable results. In addition, we keep full access to the dependences on all details of the microscopic interaction potentials, which are essential for the understanding of wetting phenomena.[1]

Moreover, we also analyze the implications of our results when they are extended into the aforementioned critical region around T_c. These particular findings must be regarded as a lowest-order estimate for those which would follow from a more complete theory incorporating the bulk critical phenomena. However, up to now such a complete theory for both bulk critical phenomena and wetting phenomena, including microscopic details, does not exist. It may be that the replacement of classical values of critical exponents by the correct three-dimensional ones improves our expressions within the critical region. But this does not incorporate the bulk critical phenomena systematically.

Thus at present this is the most adequate, manageable approach for the problem under consideration. Only numerical simulations thereof (see Sec. III D in Ref. 1 for a list of relevant references) seem to require less approximations. However, all of them are restricted to the study of systems with basically short-range forces. Even with special purpose computers the finite size of the simulated systems requires a cutoff of the interaction potentials at 2.5σ, where σ is the hard-core diameter of the fluid particles.[13] Consequently, such an approach necessarily misses just those long-range features that are of crucial importance for the wetting behavior in fluids. Moreover, these simulations are again applicable only for a very small subset of interaction parameters.

II. WETTING OF A WALL BY A ONE-COMPONENT FLUID

According to the Introduction the interface between a solid wall and the gas phase of a simple one-component fluid may be wetted by the liquid phase via complete wetting upon approaching the gas-liquid coexistence curve $\mu_0(T)$ from the gas side $\mu<\mu_0(T)$ or via critical or first-order wetting upon approaching T_c along the gas side of the gas-liquid coexistence curve. These kinds of interfacial phase transitions at a wall are not only of great experimental and technical importance but they offer also a particularly clear and transparent statement of the theoretical problem because the position of the α-γ interface is prescribed and fixed geometrically.

A. Density functional

As stated in Sec. I we start from the following density functional for inhomogeneous fluid systems:[11,1-3,14]

$$\begin{aligned}\Omega[\{\rho(\mathbf{r})\};T,\mu;\{w(|\mathbf{r}-\mathbf{r}'|)\},\{V(\mathbf{r})\}] &= \int d^3r\, f_h(\rho(\mathbf{r}),T) \\ &+ \tfrac{1}{2}\int d^3r \int d^3r'\, \tilde{w}(|\mathbf{r}-\mathbf{r}'|)\rho(\mathbf{r})\rho(\mathbf{r}') \\ &+ \int d^3r\,[\rho_w V(\mathbf{r})-\mu]\rho(\mathbf{r})\ . \qquad (2.1)\end{aligned}$$

$\Omega[\{\rho(\mathbf{r})\};T,\mu]$ is the grand canonical potential for a given number density $\rho(\mathbf{r})$ of the fluid, which is confined to the half-space $V_+=\{\mathbf{r}=(\mathbf{r}_\parallel,z)\in\mathbb{R}^3|z\geq 0\}$. The fluid particles interact via spherically symmetric pair potential $w(r)$, which are attractive at large distances r where they decay $\sim r^{-6}$. Their divergent repulsive part at small distances is treated by the introduction of a reference system of hard spheres with diameter r_0. $f_h(\rho,T)$ is the bulk Helmholtz free-energy density of a homogeneous reference system with number density ρ. According to the Weeks-Chandler-Andersen theory[15] one has $\tilde{w}(r\geq\bar{r}_0)=w(r)$ where $\bar{r}_0$ is the position of the minimum of $w(r)$; $\tilde{w}(r\leq\bar{r}_0)=w(\bar{r}_0)=\tilde{w}(\bar{r}_0)$. The optimum choice for the hard-sphere diameter r_0 is determined by a certain correlation function. It depends on $\{w(r\leq\bar{r}_0)\}$, the mean density ρ, and temperature T.[15] In our subsequent discussion of the effective interace potential $\Omega_s(l)$ for thick wetting films neither the explicit form of $\tilde{w}(r<\bar{r}_0)$ nor of $f_h(\rho,T)$ will enter. Therefore we do not embark further into these details and we only state that Eq. (2.1) is uniquely determined by the interaction $w(r)$ between the fluid particles and the substrate potential $\rho_w V(\mathbf{r})$. For convenience in the latter one we introduce the mean number density ρ_w of the wall. Since the corrugation effects in the substrate potential decay exponentially[16] and since we are interested in the power-law behavior of $\Omega_s(l)-\Omega_s(\infty)$ for large l we ignore the dependence of V on $\mathbf{r}_\parallel$ so that $V(\mathbf{r})\equiv V(z)$. Consequently, the actual density profile $\rho_0[z;T,\mu;\{w(r)\},\{V(z)\}]$, which minimizes

$\Omega[\{\rho(\mathbf{r})\};T,\mu]$ for a given boundary condition at $z=+\infty$, depends on the spatial variables only through the distance z from the wall. The wall occupies the half-space $V_-=\{\mathbf{r}\in\mathbb{R}^3|z\le 0\}$ so that $V(z)\sim z^{-3}$ for large z. $z=0$ is given by the mean position of the nuclei of the top substrate layer. Thus the fluid density vanishes for $z\lesssim d_w$ where d_w is given by the sum of the radii of the fluid particles and of the substrate particles.[17,8] The actual grand canonical potential $\Omega[T,\mu,\{w(r)\},\{V(z)\}]$ is the minimum value of Eq. (2.1) at $\rho(\mathbf{r})=\rho_0[z;T,\mu;\{w(r)\},\{V(z)\}]$.

Before we proceed let us briefly mention the limitations of Eq. (2.1). First, as mentioned in the Introduction, it yields classical critical exponents near T_c. Second, Eq. (2.1) does not allow for the formation of a solid phase. In the derivation of Eq. (2.1) the two-particle density of the reference system is replaced by its asymptotic form $\rho(\mathbf{r})\rho(\mathbf{r}')$ for $|\mathbf{r}-\mathbf{r}'|\to\infty$ and the free energy of the inhomogeneous reference system is evaluated in the local-density approximation by using the free-energy density for a homogeneous reference fluid. As an approximate analytic expression for $f_h(\rho,T)$ one may adopt the Percus-Yevick formula[18,15] or the Carnahan-Starling[19,15] formula, which, however, are not capable of describing the freezing transition of the hard-sphere reference system. (Up to now no analytic expression for this freezing transition is known.) Here, however, we focus only on fluid phases, i.e., $T>T_t$. Thus in our context the main deficiency of Eq. (2.1) consists in the absence of density oscillations near the wall caused by packing effects (see Sec. III B of Ref. 1 for a list of the relevant references). Here we ignore them because we are interested in the algebraic decay of $\Omega_s(l)-\Omega_s(\infty)$ for large l and because these density oscillations decay exponentially even in the presence of long-range van der Waals interactions.[20] This is a reasonable approximation for the continuous wetting transitions we are considering here. However, in the case of first-order wetting transitions, for which the behavior $\Omega_s(l)$ at small values of l may be important, it is indispensable to take these density oscillations into account.[21,22] The application of the weighted density-functional theory[23] to inhomogeneous systems may prove to be a promising way to solve such problems.

B. Structure of the wall-fluid interface

According to our general approach described in the Introduction we want to understand the wall-gas interface, which includes a thick liquidlike layer, in terms of the emerging free wall-liquid and liquid-gas interfaces. Thus in the following we describe briefly the predictions of Eq. (2.1) for the latter two interfacial structures.

Let us first separate Eq. (2.1) into the bulk contribution $\sim V_+$ and into the surface contribution $\sim A$, where A is the surface area of the wall,

$$\Omega[\{\rho(z)\};T,\mu;\{w(r)\},\{V(z)\}]=V_+\Omega_b[\rho_\gamma;T,\mu;\{w(r)\}]+A\,\Omega_s[\{\rho(z)\};T,\mu;\{w(r)\},\{V(z)\}]\,, \tag{2.2}$$

where

$$\Omega_b[\rho;T,\mu;\{w(r)\}]=f_h(\rho,T)+\tfrac{1}{2}w_0\rho^2-\mu\rho \tag{2.3}$$

and

$$w_0=\int_{-\infty}^{\infty}dz\,\hat{w}(z)\,, \tag{2.4}$$

with

$$\hat{w}(z)=\int d^2r_\parallel\,\tilde{w}[(\mathbf{r}_\parallel^2+z^2)^{1/2}]\,. \tag{2.5}$$

(Recall that $\tilde{w}$ and the hard-core diameter r_0 entering f_h are determined by w.) Equation (2.2) holds for all density profiles which attain the constant value ρ_γ for $z\to+\infty$ rapidly enough so that the integrals, which determine $\Omega_s[\{\rho(z)\}]$, exist. Under this condition one obtains

$$\Omega_s^{(\gamma)}[\{\rho(z)\};T,\mu;\{w(r)\},\{V(z)\}]=\int_0^\infty dz\,[f_h(\rho(z),T)-f_h(\rho_\gamma,T)]+\tfrac{1}{2}\int_0^\infty dz\int_0^\infty dz'\hat{w}(|z-z'|)\delta\rho_\gamma(z)\delta\rho_\gamma(z')+\int_0^\infty dz(\rho_\gamma w_0-\mu)\delta\rho_\gamma(z)-\rho_\gamma\int_0^\infty dz\,t(z)\delta\rho_\gamma(z)-\tfrac{1}{2}\rho_\gamma^2\int_0^\infty dz\,t(z)+\rho_w\int_0^\infty dz\,V(z)\rho(z)\,, \tag{2.6}$$

with $\delta\rho_\gamma(z)=\rho(z)-\rho_\gamma$ and

$$t(z)=\int_z^\infty dz'\hat{w}(z')\,. \tag{2.7}$$

Note that $w_0=2t(0)$ and that we consider only such density profiles $\rho(z)$ which vanish rapidly enough for $z\to 0$ so that the last integral in Eq. (2.6) exists. For given values of μ and T the actual bulk density $\rho_0(T,\mu;w_0,r_0)$ minimizes Eq. (2.3) and yields the bulk grand potential. For $\mu\le\mu_0(T)$ ρ_γ is the gas density ρ_g and for $\mu\ge\mu_0(T)$ it is the liquid density ρ_l.

Thus for $\mu\ge\mu_0(T)$ and $\rho_\gamma=\rho_l$ the wall-liquid surface tension σ_{wl} is the minimum of Ω_s:

$$\sigma_{wl}[T,\mu;\{w(r)\},\{V(z)\}]=\min_{\{\rho(z)\}}\Omega_s^{(l)}[\{\rho(z)\};T,\mu;\{w(r)\},\{V(z)\}]\,. \tag{2.8}$$

Indeed $\delta\Omega_s^{(\gamma)}[\{\rho(z)\}]/\delta\rho(z)=0$ leads to the known integral equation for the actual wall-liquid interface profile $\rho_{wl}[z;T,\mu;\{w(r)\},\{V(z)\}]$:

$$\mu=\frac{\partial f_h}{\partial\rho}(\rho_{wl}(z),T)+\int_0^\infty dz'\hat{w}(|z-z'|)\rho_{wl}(z')+\rho_w V(z)\,. \tag{2.9}$$

Similarly for $\mu\le\mu_0(T)$ and with $\rho_\gamma=\rho_g$ Eq. (2.6) yields the wall-gas surface tension σ_{wg} and the actual wall-gas

interface profile $\rho_{wg}[z;T,\mu;\{w(r)\},\{V(z)\}]$. Figure 1(a) shows the qualitative behavior of $\rho_{wl}(z)$ as the solution of Eq. (2.9). For $z\to 0$ $V(z)$ diverges and $\rho_{wl}(z)$ vanishes. In this limit Eq. (2.9) yields

$$\rho_{wl}(z)\sim\exp[-\rho_w V(z)/(k_B T)] \ . \tag{2.10}$$

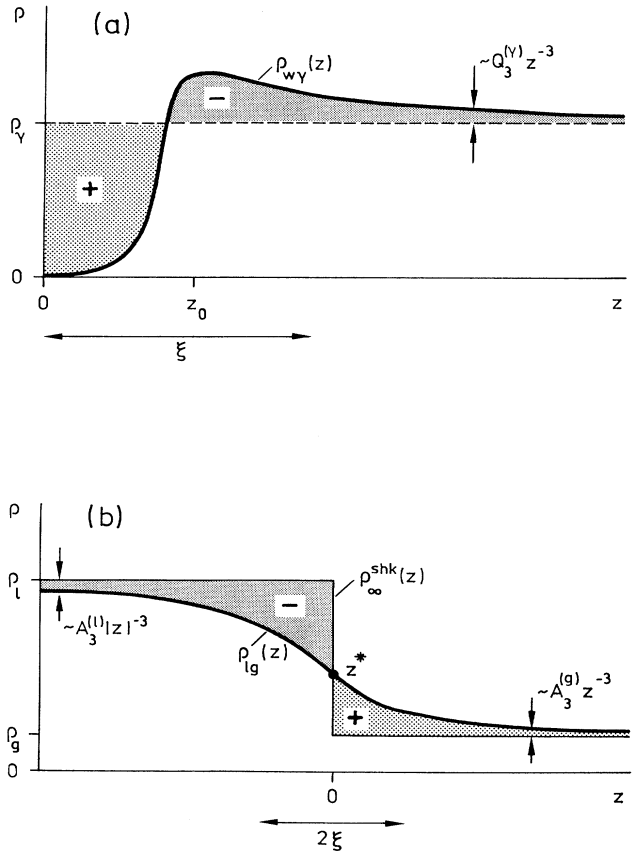

FIG. 1. Qualitative behavior of the wall-fluid interface profile (a) $\rho_{w\gamma}(z)$ and of the free liquid-gas interface profile (b) $\rho_{lg}(z)$. In (a) $\rho_{w\gamma}(z)$ vanishes for $z\to 0$ with an essential singularity, reaches a maximum at $z=\bar{z}_0$, which may coincide with the minimum of $V(z)$, and decays $\sim Q_3^{(\gamma)} z^{-3}$ towards the bulk value ρ_γ at $z=+\infty$ with $\gamma=l$ or g. The asymptotic behavior of $\rho_{w\gamma}(z)$ starts for $z\gtrsim\xi$. $Q_3^{(\gamma)}$ can also be negative so that $\rho_{w\gamma}(z)$ approaches ρ_γ from below (see Fig. 2). In (b) $\rho_{lg}(z)$ reaches ρ_l as $A_3^{(l)}|z|^{-3}$ for $z\to-\infty$ and ρ_g as $A_3^{(g)} z^{-3}$ for $z\to+\infty$. The main variation of $\rho_{lg}(z)$ occurs in a slab of thickness 2ξ around its center z^* located at $z=0$. $\rho_\infty^{shk}(z)=\rho_l\Theta(-z)+\rho_g\Theta(z)$ is the sharp-kink approximation for $\rho_{lg}(z)$. For $T\to T_c$ ξ diverges both in (a) and (b), $\rho_\gamma\to\rho_c$, and $\rho_l-\rho_g\to 0$. The coefficients $A_3^{(\gamma)}$ are always positive. In (a) and for $\gamma=l$ the difference between the positively and the negatively marked area divided by ρ_l is a microscopic length $d_{wl}^{(1)}$ which enters the coefficients of the effective interface potential [cf. Eq. (2.36)]. In (b) the difference between the positively and the negatively marked area divided by $\rho_l-\rho_g$ is a microscopic length $d_{lg}^{(1)}$ corresponding to the free liquid-gas interface [cf. Eq. (2.37)]. The value of $d_{wl}^{(1)}$ is uniquely fixed, whereas $d_{lg}^{(1)}$ depends on the choice of z^*.

For a strong substrate potential $\rho_{wl}(z)$ rises above ρ_l and finally approaches ρ_l for $z\to\infty$ from above. Thus $\rho_{wl}(z)$ can be represented as

$$\rho_{wl}(z)=\begin{cases} q(z), & z\le\xi \\ \rho_l+\sum_{k=3}^{\infty} Q_k^{(l)} z^{-k}, & z\ge\xi \ . \end{cases} \tag{2.11}$$

Here, without further specification, $q(z)$ describes the variation of $\rho_{wl}(z)$ close to the wall. For z larger than ξ, which is proportional to the bulk correlation length, $\rho_{wl}(z)$ approaches ρ_l via van der Waals tails.

This latter behavior can be confirmed by analyzing Eq. (2.9) along the lines of Ref. 24. As an exact result one finds

$$Q_3^{(l)}=\rho_l^2(\rho_w u_3-\rho_l t_3)\kappa_T^{(l)} \ . \tag{2.12}$$

Here $\kappa_T^{(l)}$ is the isothermal compressibility $VN^{-2}(\partial N/\partial\mu)_{T,V}=-V^{-1}(\partial V/\partial p)_{T,N}$ of the liquid with $\rho_l=\rho_l(\mu,T)$ (p is the pressure and N is the mean number of particles):

$$\kappa_T^{(l)}=\rho_l^{-2}\left[\frac{\partial^2 f_h}{\partial\rho^2}(\rho_l,T)+w_0\right]^{-1} \ . \tag{2.13}$$

u_3 and t_3 characterize the leading asymptotic behavior of the substrate potential and the fluid-fluid interaction, respectively:

$$V(z)=-\sum_{k\ge 3} u_k z^{-k}, \quad z\gg\bar{z}_0 \tag{2.14}$$

where $\bar{z}_0$ is the position of the minimum of $V(z)$ and

$$t(z)=-\sum_{k\ge 3} t_k z^{-k}, \quad z\gg\bar{r}_0 \ . \tag{2.15}$$

Note that $Q_3^{(l)}$ is dimensionless and diverges, within mean-field theory, $\sim t^{-1}$ for $t=(T_c-T)/T_c\to 0$ along the coexistence line $\mu_0(T)$. Nonetheless these van der Waals tails become irrelevant close to T_c since $Q_3^{(l)} z^{-3}<Q_3^{(l)}\xi^{-3}\sim t^{-1}t^{+3/2}\sim t^{1/2}\to 0$. This must be the case because near T_c the long-range van der Waals interactions $\sim r^{-6}$ as well as all subdominant power-law contributions are irrelevant compared with short-range forces.[25] In addition, for $\xi\to\infty$ also the power-law contributions of $V(z)$, i.e., all u_k with $k\ge 3$, become irrelevant, because close to T_c, in the sense of the renormalization-group theory, $V(z)$ is equivalent to a localized surface field $\sim\delta(z)$.[26] At T_c *critical adsorption* occurs such that $\rho_{wl}(z)-\rho_c\sim z^{-1}$ for $z\to\infty$ within mean-field theory. In general, one finds $\rho_{wl}-\rho_c\sim z^{-\beta/\nu}$ where $\beta\simeq 0.33$ and $\nu\simeq 0.63$ are the standard bulk critical exponents.[26] This shows again that at T_c the van der Waals tails $\sim z^{-3}$ are irrelevant compared with the decay $\sim z^{-\beta/\nu}$ of the critical density profile. (On the gas side critical adsorption means that the equilibrium thickness of the wetting layer is proportional to the diverging bulk correlation length.)

At this stage it is interesting to compare Eq. (2.12), which holds on the liquid side of the coexistence line $\mu_0(T)$, with the effective interface potential $\Omega_s(l)$ for the

restricted wall-gas interface, which is valid on the gas side of $\mu_0(T)$. At coexistence one has[1] [cf. Eqs. (2.29) and (2.30)]

$$\Omega_s(l)=\sigma_{wl}+\sigma_{lg}+\omega(l) , \tag{2.16}$$

with

$$\omega(l)=\sum_{k\geq 2} a_k l^{-k} \tag{2.17}$$

for $l>\xi$. One finds with $\Delta\rho=\rho_l-\rho_g$

$$a_2=\tfrac{1}{2}\Delta\rho(\rho_w u_3-\rho_l t_3) . \tag{2.18}$$

We shall show later that Eq. (2.18) is an exact expression for the leading term of the effective interface potential [cf. Eq. (2.31)]. Thus the asymptotic behavior of the wall-liquid interface profile can be expressed in terms of the asymptotic behavior of the effective interface potential for the restricted wall-gas surface tension:

$$Q_3^{(l)}=2(\rho_l-\rho_g)^{-1}\rho_l^2\kappa_T^{(l)}a_2 . \tag{2.19}$$

Note that $Q_3^{(l)}$ and a_2 have the same sign and that the important factor $\rho_w u_3-\rho_l t_3$, which determines this sign, can vary between its minimum value $\rho_w u_3-\rho_l t_3$ and its maximum value $\rho_w u_3-\rho_c t_3$ where ρ_{lt} and ρ_c are the liquid densities at the triple point T_t and at T_c, respectively. Thus for $u_3/t_3<\rho_c/\rho_w$, a_2 and $Q_3^{(l)}$ are negative for all temperatures $T_t\leq T<T_c$. (Since we are considering only van der Waals interactions t_3 must be positive.) In this case $a_2<0$, thus $l=\infty$ is always a maximum of $\Omega_s(l)$ and wetting on the gas side can never occur. Instead, a drying transition on the liquid side of $\mu_0(T)$ is possible. This checks with the fact $Q_3^{(l)}<0$. In this case $\rho_{wl}(z)$ approaches ρ_l from below, because the wall prefers the gas phase. If $u_3/t_3>\rho_{lt}/\rho_w$, $Q_3^{(l)}$ is positive for all temperatures, which reflects the fact that a strong substrate potential prefers the liquid phase. Since in this case $a_2>0$ one can conclude that, if the wall-liquid density profile approaches ρ_l from above, the system is either wet on the gas side of $\mu_0(T)$ for all temperatures or it undergoes a first-order wetting transition.[1] If, however, $\rho_c/\rho_w<u_3/t_3<\rho_{lt}/\rho_w$, a_2 is negative at T_t and positive close to T_c. Thus there exists a temperature T_w with $T_t<T_w<T_c$ such that $a_2(T=T_w)=0$. If, in addition, $a_3(T_w)>0$, T_w is indeed the transition temperature for a continuous wetting transition.[1]

Equation (2.12) therefore states that for a continuous wetting transition to occur the wall-liquid density profile must approach ρ_l from below at the triple point and from above close to T_c. Thus we obtain the surprising result that critical wetting on the *gas side* of $\mu_0(T)$ goes along with a change of sign for the asymptotic behavior of the wall-liquid density profile on the *liquid side* of $\mu_0(T)$. This change of sign occurs at the wetting transition temperature T_w. Above T_w the wall prefers the liquid phase and $Q_3^{(l)}>0$ whereas $Q_3^{(l)}<0$ below T_w.

Since drying and wetting transitions are complementary—either one has $\sigma_{wg}=\sigma_{wl}+\sigma_{lg}$ or $\sigma_{wl}=\sigma_{wg}+\sigma_{gl}$ but not both—and because they can be mapped onto each other by suitable choices of the interaction parameters (see above and Ref. 27) in the following we concentrate on the wetting phenomena. Thus we take $\mu\leq\mu_0(T)$ so that σ_{wl} is nonsingular. In Fig. 2 we summarize our findings for the asymptotic behavior of the wall-fluid interface profile. There we also include a discussion of the wall-gas interface. The same arguments as above show that

$$\sigma_{wg}(z\to\infty)=\rho_g+Q_3^{(g)}z^{-3}+\cdots , \tag{2.20}$$

with

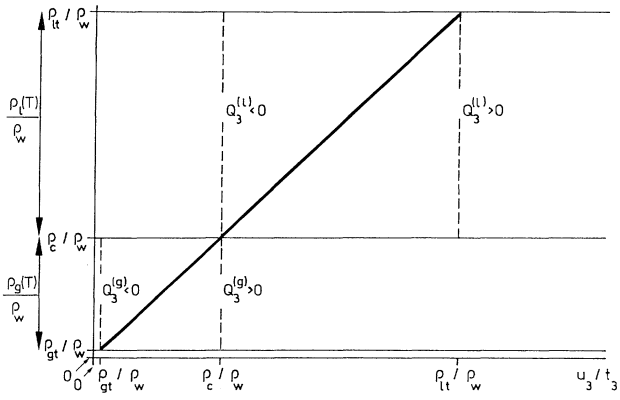

FIG. 2. Asymptotic behavior of the wall-fluid interface profile, $\rho_{w\gamma}(z\to\infty)=\rho_\gamma+Q_3^{(\gamma)}z^{-3}+\cdots$, as a function of the asymptotic strength u_3 of the substrate potential. $\rho_g(T)$ varies between $\rho_{gt}=\rho_g(T=T_t)$ and $\rho_c=\rho_g(T=T_c)=\rho_l(T=T_c)$ and $\rho_l(T)$ varies between ρ_c and $\rho_{lt}=\rho_l(T=T_t)$. Here the asymptotic strength t_3 of the fluid-fluid interaction is kept constant so that ρ_{lt}, ρ_c, and ρ_{gt} are independent of u_3/t_3. All densities are measured in units of the mean number density ρ_w of the wall, which is taken to be independent of u_3. Here we take $\rho_c/\rho_{lt}\simeq 0.35$ as obtained for Lennard-Jones systems (Ref. 23). For reasons of visibility we choose ρ_{gt}/ρ_c much larger than it is in reality; $T_t/T_c\simeq 0.5$ (Ref. 23). On the left from the diagonal $Q_3^{(\gamma)}$ is negative for both $\gamma=l$ and $\gamma=g$, i.e., $\rho_{w\gamma}(z)$ approaches ρ_γ from below. On the right from the diagonal $Q_3^{(\gamma)}$ is positive so that $\rho_{w\gamma}(z)$ approaches $\rho_\gamma(z)$ from above. This is the case for a strong substrate potential. In order to achieve this latter behavior the substrate potential has to be less strong for the wall-gas interface than for the wall-liquid interface. For $u_3/t_3>\rho_{lt}/\rho_w$ as well as for $u_3/t_3<\rho_c/\rho_w$ $Q_3^{(l)}$ does not change sign as a function of temperature. $Q_3^{(g)}$ also does not change sign if $u_3/t_3>\rho_c/\rho_w$ or $u_3/t_3<\rho_{gt}/\rho_w$. In the window $\rho_c/\rho_w<u_3/t_3<\rho_{lt}/\rho_w$ $Q_3^{(l)}$ changes sign as a function of temperature and so does $Q_3^{(g)}$ for $\rho_{gt}/\rho_w<u_3/t_3<\rho_c/\rho_w$. Within these ranges $Q_3^{(l)}$ becomes positive and $Q_3^{(g)}$ negative upon an increase of temperature. The temperature at which $Q_3^{(l)}$ of the wall-liquid interface changes sign coincides with the transition temperature of critical wetting of the wall-gas interface. $Q_3^{(g)}$ of the wall-gas interface changes sign at the critical drying transition of the wall-liquid interface. $Q_3^{(l)}<0$ implies that the wall-gas interface is nonwet, whereas $Q_3^{(l)}>0$ implies either that the wall-gas interface is wet or that it may undergo a first-order wetting transition at a temperature higher than that given by the diagonal.

$$Q_3^{(g)}=\rho_g^2(\rho_w u_3-\rho_g t_3)\kappa_T^{(g)} , \tag{2.21}$$

where $\kappa_T^{(g)}$ is the isothermal compressibility of the gas phase [see Eq. (2.13)]. Note that Eq. (2.20) holds quite generally even in the presence of a wetting film with arbitrary but finite thickness l.

In Eq. (2.11) we omitted additional exponential contributions to $\rho_{wl}(z\geq\xi)$ because later we shall use Eq. (2.11) for computing the algebraic decay of $\omega(l)$. In this respect exponential tails are irrelevant. Finally we note that in reality there are density oscillations around the van der Waals tail of $\rho_{w\gamma}(z)$ whose envelope decays exponentially.[20] As already discussed Eq. (2.1) does not exhibit these structures and we ignore them here. The leading asymptotic behavior of the effective interface potential and the values of $Q_3^{(\gamma)}$ are independent of this fine structure at the wall.

C. Structure of the liquid-gas interface

Let us now consider the free liquid-gas interface along the gas-liquid coexistence curve $\mu=\mu_0(T)$. For this case in Eq. (2.1) $V(\mathbf{r})\equiv 0$, all integrals extend over the whole space $\mathbb{R}^3$, and we impose the boundary conditions $\rho(z=-\infty)=\rho_l$ and $\rho(z=+\infty)=\rho_g$. Then one obtains

$$\begin{aligned}\Omega_s^{(\infty)}[\{\rho(z)\};T;\{w(r)\}]=&\int_{-\infty}^{\infty}dz\,[f_h(\rho(z),T)-f_h(\rho_\infty^{shk}(z),T)]+\tfrac{1}{2}\int_{-\infty}^{\infty}dz\int_{-\infty}^{\infty}dz'\hat{w}(|z-z'|)\delta\rho_\infty(z)\delta\rho_\infty(z')\\&+\int_{-\infty}^{\infty}dz[w_0\rho_\infty^{shk}(z)-\mu_0(T)]\delta\rho_\infty(z)+\Delta\rho\int_{-\infty}^{\infty}dz\,[\mathrm{sgn}(z)]t(|z|)\delta\rho_\infty(z)\\&-\tfrac{1}{2}(\Delta\rho)^2\int_0^{\infty}dz\,t(z) ,\end{aligned} \tag{2.22}$$

with $\Delta\rho=\rho_l-\rho_g$, $\delta\rho_\infty(z)=\rho(z)-\rho_\infty^{shk}(z)$; $\rho_\infty^{shk}(z)=\Theta(z)\rho_g+\Theta(-z)\rho_l$ is the sharp-kink approximation for the free interface. The actual liquid-gas interface profile $\rho_{lg}[z;T;\{w(r)\}]$ minimizes Eq. (2.22) and renders the liquid-gas surface tension $\sigma_{lg}[T;\{w(r)\}]$. Note that for any z_0 one has

$$\Omega_s^{(\infty)}[\{\rho(z)\};T;\{w(r)\}]=\Omega_s^{(\infty)}[\{\rho(z+z_0)\};T;\{w(r)\}] .$$

Correspondingly the position of the free interface profile is not fixed.

Figure 1(b) shows the qualitative behavior of the free liquid-gas interface. $\rho_{lg}(z)$ varies smoothly between ρ_l at $z=-\infty$ and ρ_g at $z=+\infty$, $\rho_\infty^{shk}(z)$ is a step function at $z=0$ taking on the value ρ_l for $z<0$ and ρ_g for $z>0$. The main variation of $\rho_{lg}(z)$ occurs within a slab of thickness 2ξ around its center. 2ξ may be taken to be the distance between the two extrema of the second derivative of $\rho_{lg}(z)$. ξ is proportional to the bulk correlation length and diverges $\sim t^{-\nu}$ for $t=(T_c-T)/T_c\to 0$. $\Delta\rho$ vanishes $\sim t^{\beta}$; within mean-field theory $\beta=\nu=0.5$. We call that point z^* of the interface profile with coordinate $z=0$ the center of the interface. According to what we said above *any* point of the interface can become its center upon a constant shift of the z coordinate without changing the form of ρ_{lg}. There are several natural choices for z^*:

$$\rho_{lg}(z=z^*)=(\rho_g+\rho_l)/2 ,$$

$$d^2\rho_{lg}(z=z^*)/dz^2=0 ,$$

or

$$\int_{-\infty}^{\infty}dz[\rho_{lg}(z)-\rho_\infty^{shk}(z)]=0 .$$

For the latter choice z^* is called the position of the equimolar dividing surface.[28] For $t\to 0$ the central part of the profile, i.e., for $|z|<\xi$, takes on a universal form which within mean-field theory is given by $\rho_{lg}(z)=\frac{1}{2}(\rho_g+\rho_l)-\frac{1}{2}\Delta\rho\tanh[z/(2\xi)]$. Outside the central part, i.e., for $|z|>\xi$, $\rho_{lg}(z)$ attains its bulk values according to inverse power laws (see Ref. 24 and Sec. IV A in Ref. 1 for a complete list of references). These portions of the interface profile are known as *van der Waals tails*, because they are induced by the presence of the van der Waals interactions. This leads to the following form of the liquid-gas interface profile:

$$\rho_{lg}(z)=\begin{cases}\rho_l-\sum\limits_{k\geq 3}A_k^{(l)}|z|^{-k}, & z\leq-\xi\\ F(z), & |z|\leq\xi\\ \rho_g+\sum\limits_{k\geq 3}A_k^{(g)}|z|^{-k}, & z\geq\xi .\end{cases} \tag{2.23}$$

Without further specification $F(z)$ describes the variation of $\rho_{lg}(z)$ around its center. Similarly as for $\rho_{wl}(z)$ exponential contributions for $|z|\geq\xi$ have been omitted here. The coefficients $A_3^{(\gamma)}$ can be inferred directly from the integral equation for $\rho_{lg}(z)$:

$$\begin{aligned}\mu_0(T)=&\frac{\partial f_h}{\partial\rho}(\rho_{lg}(z),T)\\&+\int_{-\infty}^{\infty}dz'\hat{w}(|z-z'|)\rho_{lg}(z') .\end{aligned} \tag{2.24}$$

One obtains

$$A_3^{(\gamma)}=\rho_\gamma^2(\rho_l-\rho_g)\kappa_T^{(\gamma)}t_3>0 , \tag{2.25}$$

where $\kappa_T^{(\gamma)}$ is given by Eq. (2.13) for $\gamma=l$ and $\gamma=g$, respectively, at $\mu=\mu_0(T)$. Equation (2.25) is in accordance with the results obtained in Ref. 24 and it follows by applying the same kind of arguments. Note that Eq. (2.25) is generally valid and it does not depend on a particular and explicit choice for the form of $\hat{w}$ as it has been used in Ref. 24. The coefficients $A_3^{(\gamma)}$ are dimensionless and upon approaching T_c along $\mu_0(T)$ they diverge $\sim t^{-1/2}$ compared with t^{-1} for $Q_3^{(\gamma)}$. Nonetheless they are also irrelevant close to T_c, because $A_3^{(\gamma)}|z|^{-3}$

$\leq A_3^{(\gamma)}\xi^{-3}\sim t\to 0$. This is also true for all subdominant power-law contributions. Finally one should note that all coefficients $A_k^{(\gamma)}$ with $k\geq 4$ depend on the choice of the center of the interface (see Appendix A). (Unfortunately, the expressions for A_4 and B_4 given in Ref. 24 are not accompanied by such a defining statement.)

D. Effective interface potential for wetting of the wall-gas interface

In Secs. II B and II C we discussed the structures of the wall-liquid and of the liquid-gas interface, which emerge from the wall-gas interface if a wetting transition occurs. In the spirit of the Introduction we now use the wall-liquid density profile $\rho_{wl}(z)$ and the liquid-gas density profile $\rho_{lg}(z)$ in order to construct the wall-gas surface tension under the restriction that at the wall a liquidlike layer of thickness l is present. We approximate this restricted surface tension, called effective interface potential $\Omega_s[l,T,\mu;\{w(r)\},\{V(z)\}]\equiv\Omega_s(l)$, by evaluating in Eq. (2.6) $\Omega_s^{(\gamma)}$ for the following density profile:

$$\rho(z,l;T)=\begin{cases}\rho_{wl}(z), & z\leq\kappa(l)-\lambda(l)\\ G(\kappa(l)-z,l), & \kappa(l)-\lambda(l)\leq z\leq\kappa(l)+\lambda(l)\\ \rho_{lg}(z-l), & z\geq\kappa(l)+\lambda(l)\ .\end{cases} \tag{2.26}$$

The behavior of $\rho(z,l;T)$ is described in Fig. 3. $\rho(z,l)$ consists of the free liquid-gas interface, whose center z^* is positioned at $z=l$, and the wall-liquid interface near the wall. They match smoothly in a transition region of width $2\lambda(l)$, which is described by an unspecified function $G(z,l)$. Since for large l the wall-liquid interface must emerge, the position of the transition region has to move to infinity, too. Therefore we choose $\kappa(l\to\infty)\sim\kappa_0 l$ with $0<\kappa_0<1$. Since the difference between the van der Waals tail of ρ_{wl} and the liquid van der Waals tails of ρ_{lg} vanishes for $l\to\infty$ we assume that also the width of the transition region vanishes. We take $\lambda(l\to\infty)\sim l^{-(1+\epsilon)}$ with $\epsilon>0$. In Appendix A we discuss weak restrictions on the form of $\kappa(l)$ and $\lambda(l)$ which ensure that

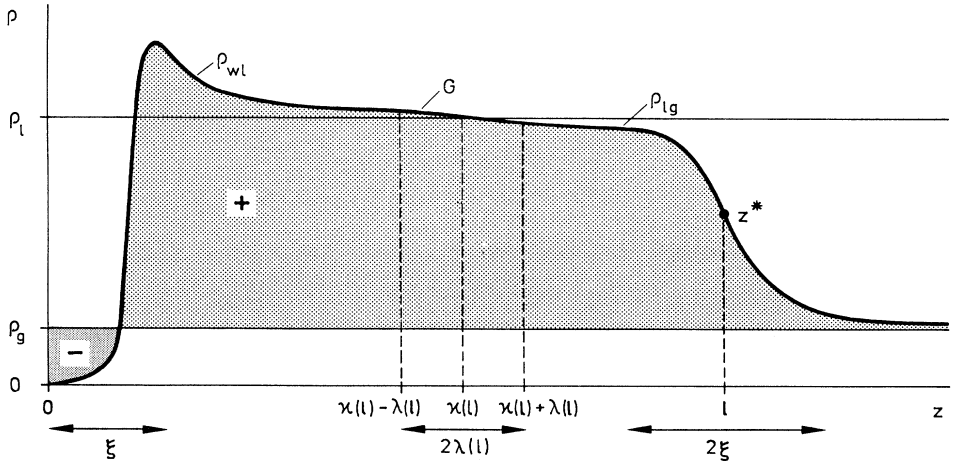

FIG. 3. Schematic drawing of the density profile $\rho(z;l)$ from Eq. (2.26) for constructing the effective interface potential $\Omega_s(l)$. The wall-liquid interface profile $\rho_{wl}(z)$ is followed by a transition region described by $G(z)$ beyond which the liquid-gas interface profile starts. The center z^* of the latter one is positioned at $z=l$. The position $z=\kappa(l)$ of the transition region grows with l because for $l\to\infty$ the wall-liquid interface profile must emerge. Thus we take $\kappa(l\to\infty)\sim l$. We further assume that $\lambda(l)$ shrinks for large l, because the difference between the van der Waals tail of ρ_{wl} and the liquid van der Waals tail of ρ_{lg} vanishes for large l; we take $\lambda(l\to\infty)\sim l^{-(1+\epsilon)}$ with $\epsilon>0$. ϵ and G are without further specification. Slight restrictions on the form of $\lambda(l)$ and $\kappa(l)$ are discussed in Appendix A. For the l dependence of G see Appendix B. Thus one may choose κ such that $\rho(z=\kappa l;l)=\rho_l$ but one is not obliged to do so. In particular, it may be that ρ_{wl} approaches ρ_l from below. As for any given density profile the value l of the thickness of the wetting film depends on a particular definition; the surface tension for this profile is independent from this definition. Here, the thickness l is fixed by the position of the center z^* of the free interface profile and thus it is tied to the definition of the center of the latter one [see Fig. 1(b)]. If in Fig. 1(b) one chooses a point z'^* with z coordinate Δz (recall that the z coordinate of z^* is 0) as a new center, the corresponding new thickness of the same wetting film will be $l'=l+\Delta z$. We shall show that the results for Ω_s are invariant with respect to such choices because Ω_s can be expressed in terms of the unique coverage $\Gamma=\int_0^\infty dz\,[\rho(z)-\rho_g]$ which is the difference between the positively and the negatively marked area (see Appendix A). Note that for a given value of l we consider only such values of μ and T so that l is larger than the bulk correlation length ξ.

for a given density profile $\rho(z)$ the corresponding coverage $\Gamma=\int_0^\infty dz\,[\rho(z)-\rho_g]$ is independent from what we define to be the thickness of the wetting film described by $\rho(z)$ (see below). For the l dependence of $G(z,l)$ see Appendix B.

One should note that the evaluation of $\Omega_s^{(\gamma)}$ for the trial function in Eq. (2.26) yields $\Omega_s(l)$, which is supposed to be a good approximation for the effective interface potential one would obtain by minimizing $\Omega_s^{(\gamma)}$ exactly under the restriction that the density profiles $\rho(z)$ have a certain property at $z=l$, e.g., $\rho(z=l)=(\rho_l+\rho_g)/2$ or $\rho''(z=l)=0$, etc. We approximate this exact restricted minimization problem by evaluating $\Omega_s^{(\gamma)}$ for such a trial function that in Eq. (2.26) the center z^* [see Fig. 1(b)] of $\rho_{lg}(z)$ is chosen to be that point where the particular property of $\rho(z=l)$ one has decided to pick (see above) is fulfilled. A further possible definition of $\Omega_s(l)$ is $l=\bar{l}=\Gamma/(\rho_l-\rho_g)$ so that $\Omega_s^{(\gamma)}$ is minimized under the restriction that $\rho(z)$ exhibits a certain coverage Γ. These various definitions are discussed and compared in Appendix A.

Finally we note that, as indicated in Fig. 3, for a given value of l we consider only such wetting films whose thicknesses are large compared with the bulk correlation length at coexistence:

$$l>\xi\ . \tag{2.27}$$

Equation (2.26) holds only at coexistence: $\rho_{lg}(z)$ is only defined for $\mu=\mu_0(T)$ and $\rho_{wl}(z)$ is evaluated at the liquid side $\mu_0^+(T)$ of liquid-gas coexistence. In order to be able to analyze complete wetting Eq. (2.26) must be generalized to the case $\mu<\mu_0(T)$. There is no obvious way to do this because both ρ_{wl} and ρ_{lg} do not exist for $\mu<\mu_0(T)$. In order to proceed we propose the simplest generalization:

$$\rho(z,l;T,\mu)=\rho(z,l;T)+\Theta(z-l)[\rho_g(T,\mu)-\rho_g(T,\mu_0(T))]\ . \tag{2.28}$$

Equation (2.28) fulfills the necessary condition for $z\to\infty$: $\rho(z,l;T,\mu)$ approaches the correct asymptotic gas density $\rho_g(T,\mu<\mu_0(T))<\rho_g(T,\mu=\mu_0(T))$. All other features of the density profile are taken to be identical to those of $\rho(z)$ at coexistence. As a consequence in the formulas for the effective interface potential given below only the gas density, where it shows up explicitly, is taken at the actual value of μ, whereas the liquid density is taken at $\mu=\mu_0(T)$. All expressions, which contain the van der Waals tails $A_k^{(\gamma)}$ or $Q_k^{(l)}$, are evaluated at $\mu=\mu_0(T)$. However, this is a crude approximation, which is valid only for small undersaturations $\mu-\mu_0(T)$, because according to Eq. (2.28) this $\rho(z,l;T,\mu)$ exhibits a discontinuity $\sim\rho_g(T,\mu)-\rho_g(T,\mu_0(T))$ at $z=l$. Another generalization for small undersaturation would be to continue all bulk liquid quantities entering Eq. (2.26), like, e.g., ρ_l or $\kappa_T^{(l)}$, to their metastable mean-field values at $\mu<\mu_0(T)$. But this raises the question of the reliability of these results beyond mean-field theory. Thus we proceed by applying Eq. (2.28).

The procedure is to evaluate $\Omega_s^{(g)}$ in Eq. (2.6) for $\rho(z)=\rho(z,l;T,\mu)$ by using Eqs. (2.28), (2.26), (2.23), and (2.11). In order to obtain explicit results one has to expand $\Omega_s^{(g)}[\{\rho(z)\},l;T,\mu]$ for large values of l by using Eq. (2.27). This is an extremely tedious calculation and its enormous length is prohibitive for any detailed presentation in a research paper. Thus we can only state that the general line of attack is to insert the aforementioned equations, which contain infinite series, into Eq. (2.6), to expand the expressions in Eq. (2.6), then to integrate them term by term, and finally to resum the infinite series and to order them in inverse powers of l. To our surprise we found that all the numerous contributions to a certain inverse power of l finally combine into very compact and transparent expressions. Let us now quote these results:

$$\Omega_s(l)=\sigma_{wl}^{(0)}+\sigma_{lg}+\omega(l)\ , \tag{2.29}$$

with

$$\omega(l)=(\mu_0-\mu)[\Delta\rho(l+d_{lg}^{(1)})-\rho_l d_{wl}^{(1)}]+\sum_{k=2}^{4}a_k l^{-k}+O(l^{-5}\ln l)\ . \tag{2.30}$$

First, Eq. (2.29) shows that in the limit $l\to\infty$ and at coexistence we recover, by starting from $\Omega_s^{(g)}$, the sum of the full expressions for $\sigma_{wl}^{(0)}=\Omega_s^{(l)}[\{\rho(z)=\rho_{wl}(z)\};\mu=\mu_0^+]$ and $\sigma_{lg}=\Omega_s^{(\infty)}[\{\rho(z)=\rho_{lg}(z)\}]$. Of course one must obtain this result because for an infinite thickness of the wetting film the wall-gas surface tension is the sum of the wall-liquid and the liquid-gas surface tension. But here this is a highly nontrivial check for our expanding and resumming procedure. The first term in Eq. (2.30) describes the fact that on the gas side $\mu<\mu_0$ the cost in free energy for forming a liquidlike layer, whose corresponding bulk phase is unstable, increases linearly as a function of its thickness l. At coexistence $\omega(l)$ vanishes for large l.

The explicit form of this first term in Eq. (2.30) is correct up to first order in $\mu_0-\mu$. We omitted the lengthy terms which are nonlinear in $\mu_0-\mu$ and which turn out to be linear in l, too. Consequently, in this first term in Eq. (2.30) both $\Delta\rho$ and $d_{lg}^{(1)}$ are taken at coexistence $\mu=\mu_0$. By construction ρ_l and $d_{wl}^{(1)}$ are evaluated at $\mu=\mu_0$. In deriving this first term in Eq. (2.30) we used the fact that $\rho_{lg}(z)$, which enters the trial function in Eq. (2.28), fulfills Eq. (2.24). Thus in the appropriate limit this first term in Eq. (2.30) does *not* reduce to the sharp-kink result, because $\rho_\infty^{shk}(z)$ does not fulfill Eq. (2.24).

The coefficients a_k are functions of T and μ and functionals of $\{w(r)\}$ and $\{V(z)\}$. Thus they determine the nature of the wetting transition and—in the case of critical wetting—the transition temperature T_w in terms of $\{w(r)\}$ and $\{V(z)\}$. The necessary conditions for a second-order wetting transition at $T=T_w$ and $\mu=\mu_0$ are that $a_2(T=T_t)<0$, $a_2(T=T_c)=0^+$, and $a_3(T=T_w)>0$, where T_w is defined implicitly by the equation $a_2(T=T_w)=0$ (see Fig. 3.2 in Ref. 1). Within our approach the explicit expressions of a_2, a_3, and a_4 are the following:

$$a_2=\tfrac{1}{2}\Delta\rho(\rho_w u_3-\rho_l t_3)\ , \tag{2.31}$$

$$a_3=a_3^{(0)}-2a_2 d_{lg}^{(1)}\ , \tag{2.32}$$

and

$$a_4=a_4^{(0)}-3a_3 d_{lg}^{(1)}+3a_2[d_{lg}^{(2)}-2(d_{lg}^{(1)})^2]\ , \tag{2.33}$$

with

$$a_3^{(0)}=\tfrac{1}{3}\Delta\rho[\rho_w u_4-\rho_l(t_4+3t_3 d_{wl}^{(1)})]\ , \tag{2.34}$$

and

$$a_4^{(0)}=\tfrac{1}{4}\Delta\rho[\rho_w u_5-\rho_l(t_5+4t_4 d_{wl}^{(1)}+6t_3 d_{wl}^{(2)})]\ . \tag{2.35}$$

Thus the coefficients a_k depend on those determining the substrate potential u_k and the fluid-fluid interaction t_k [see Eqs. (2.14) and (2.15)], the mean number density ρ_w of the wall, the liquid density at coexistence $\rho_l[T,\mu=\mu_0^+;\{w(r)\}]$, the gas density $\rho_g[T,\mu\le\mu_0(T);\{w(r)\}]$, as well as on moments of the wall-liquid and the free liquid-gas interface profile, respectively, both at coexistence ($i=1,2$):

$$d_{wl}^{(i)}=i\int_0^\infty dz\, z^{i-1}[1-\rho_{wl}(z)/\rho_l] \tag{2.36}$$

and

$$d_{lg}^{(i)}=\frac{i}{\Delta\rho}\int_{-\infty}^{\infty} dz\, z^{i-1}[\rho_{lg}(z)-\rho_\infty^{shk}(z)]\ . \tag{2.37}$$

$d_{wl}^{(i)}$ and $d_{lg}^{(i)}$ are functions of temperature and functionals of $\{w(r)\}$. $d_{wl}^{(i)}$ is, in addition, also a functional of $\{V(z)\}$ and depends, *inter alia*, on the behavior of the substrate potential at *all* distances. A geometrical interpretation of the lengths $d_{wl}^{(1)}$ and $d_{lg}^{(1)}$ is given in Fig. 1.

The dependence of the coefficients a_2, a_3, and a_4 on μ turns out to be rather simple. According to Eqs. (2.31)–(2.35) all three coefficients possess $\Delta\rho=\rho_l-\rho_g$ as a common prefactor. In this prefactor ρ_g is taken at its actual value $\mu\le\mu_0$ off coexistence. This is the *only* μ dependence in the coefficients a_k. It turns out that all other quantities, $d_{lg}^{(i)}$, $d_{wl}^{(i)}$, and ρ_l, have to be taken *at* coexistence $\mu=\mu_0$. These rules hold for arbitrary values of μ and not only up to first order in $\mu_0-\mu$.

Before we continue to discuss the above results let us recall that the values of $d_{lg}^{(i)}$ depend on our choice of what we call the thickness of the wetting film (see Figs. 1 and 3). In Appendix A we discuss this dependence of $\Omega_s(l)$ on the definition of l. There, in addition, we express $\omega(l)$ in terms of the coverage Γ (see Fig. 3). As it must be, this latter expression does not depend on the choice of the definition for $\omega(l)$.

One can check that Eqs. (2.30)–(2.37) contain in the corresponding limits as special cases those results which have been omitted previously within the sharp-kink[8] and soft-kink[9] approximation, respectively. The sharp-kink results follow by putting $d_{lg}^{(i)}=0$ and by replacing $d_{wl}^{(1)}$ by d_w and $d_{wl}^{(2)}$ by $(d_w)^2$. (In the soft-kink approximation the same replacements apply. In addition, $d_{lg}^{(i)}$ is nonzero and takes on its soft-kink approximation value.) Although this correspondence looks rather simple one should appreciate the superiority of our present approach. The sharp-kink approximation requires d_w and the soft-kink approximation requires both d_w and the thickness ξ of the central part of the free liquid-gas interface profile as input data which are both not uniquely specified by the theory itself. However, in our present approach it turns out that d_w and $(d_w)^2$ are replaced by uniquely specified moments of the wall-liquid interface profile [see Eq. (2.36)]. In addition, all explicit dependences on ξ [see Fig. 1 and Eqs. (2.11), (2.23), and (2.26)] drop out. Thus our expression for the effective interface potential is now indeed independent from any, in principle arbitrary, choice of input parameters of the trial function $\rho(z,l)$ [see Eq. (2.26)] and therefore it can be computed uniquely. This also implies that the first few leading terms of the effective interface potential are independent from the details of matching the wall-liquid and the liquid-gas interface profiles in order to form a continuous trial function in Eq. (2.26). We show in Appendix B that a_2, a_3, and a_4 do not depend on $G(z,l)$, $\kappa(l)$, and $\lambda(l)$.

We stress this independence for the following reason. At coexistence one has $\Omega_s(l=\infty)=\sigma_{wl}+\sigma_{lg}$. Thus by construction the value of the effective interface potential for the wall-gas interface at $l=\infty$ is determined by the wall-liquid and the liquid-gas interface profile [see Eqs. (2.6), (2.8), and (2.22)]. [Of course, in addition the knowledge of $w(r)$ and $\rho_w V(z)$ as well as of the properties of the coexisting bulk phases are required.] In the case of continuous wetting transitions the leading correction terms $\omega(l)=a_2 l^{-2}+a_3 l^{-3}+\cdots$ determine the character of the wetting transition. As already stated before the necessary conditions for the occurrence of a continuous wetting transition at $T=T_w$ are $a_2(T=T_t)<0$, $a_2(T=T_c)=0^+$, and $a_3(T=T_w)>0$.[1] The transition temperature for critical wetting is given implicitly by $a_2(T=T_w)=0$. In the latter case the equilibrium thickness l_0 of the wetting film diverges according to

$$l_0(T\to T_w,\Delta\mu=0)=\frac{3}{2}\frac{a_3}{|a_2|}\left[1+\frac{8}{9}\frac{a_4}{a_3^2}|a_2|+\cdots\right]\ , \tag{2.38}$$

whereas for complete wetting one has

$$l_0(T>T_w,\Delta\mu\to 0)=\left[\frac{2a_2}{\Delta\rho}\right]^{1/3}(\Delta\mu)^{-1/3}\left[1+\frac{a_3(\Delta\rho)^{1/3}}{(2a_2)^{4/3}}(\Delta\mu)^{1/3}+\cdots\right]\ , \tag{2.39}$$

where a_2, a_3, and $\Delta\rho$ are taken at coexistence $\mu=\mu_0$.

Higher-order wetting transitions involve the higher coefficients in the expansion of $\omega(l)$. Therefore the observed independence from the matching conditions shows within this approach the following results: (i) Besides interaction parameters and bulk densities only the wall-liquid and the liquid-gas interface profiles determine the order of the wetting transitions. (ii) In the case of con-

tinuous wetting transitions at coexistence the same quantities also determine the amplitude of the leading term in the power-law behavior of the thickness of the wetting film. These results are nontrivial because the actual density profile deviates from the superposition of the wall-liquid and liquid-gas density profiles.

As discussed above the difference between the results in Eqs. (2.31)–(2.36) and the analogous ones obtained from the sharp-kink and soft-kink approximation[8,9] reflects the importance of the van der Waals tails and of the structure of the emerging wall-liquid interface. The coefficient a_2 is independent of both features [see Eq. (2.31)] so that T_w is given by the sharp-kink result $\rho_l(T=T_w)=\rho_w u_3/t_3$, i.e., the wetting transition is induced only by the temperature dependence of the bulk liquid density.

The higher-order coefficients a_3 and a_4 do depend on both the van der Waals tails and the wall-liquid interface structure. The latter enters via the zeroth ($d_{wl}^{(1)}$) and the first moment ($d_{wl}^{(2)}$). The van der Waals tails are contained implicitly in $d_{wl}^{(i)}$ and in $d_{lg}^{(i)}$ [see Eqs. (2.35) and (2.36)]; $d_{lg}^{(1)}$ and $d_{lg}^{(2)}$ are the only terms through which the smooth variation of the center of the emerging free liquid-gas interface enters the effective interface potential. As discussed above the separatrix between first- and second-order wetting is given by $a_3(T=T_w)=0$ with $a_2(T_w)=0$ and the separatrix between first- and third-order wetting is given by $a_4(T=T_w)=0$ where $a_2(T=T_w)=a_3(T=T_w)=0$. Equations (2.31)–(2.35) show that these separatrices are *independent* from the liquid-gas interface profile, because the quantities $d_{lg}^{(1)}$ and $d_{lg}^{(2)}$ drop out at the corresponding transition temperatures [see also Eqs. (A2) and (A6)]. The separatrices depend only on the structure of the wall-liquid interface via $d_{wl}^{(i)}$ [see Eqs. (2.34) and (2.35)]. This makes the previous finding from the soft-kink approximation more specific. These findings had been that the bulk correlation length, which determines the width of the central part of the free liquid-gas interface, is irrelevant for continuous wetting transitions. Here we find that even the van der Waals tails of the free liquid-gas interface do not affect the separatrices; only the van der Waals tail of the wall-liquid interface does so. However, T_w^* of a first-order wetting transition depends on *all* van der Waals tails because it is determined by all a_k, $k \geq 2$, and because $a_2(T=T_w^*) \neq 0$.

The presence of the van der Waals tails leads to a novel feature in the asymptotic behavior of the effective interface potential. Both the sharp-kink and the soft-kink approximations predict that $\omega(l)$ can be expanded into inverse powers of l. However, the van der Waals tails lead to additional logarithmic terms $\sim l^{-5}\ln l$ which have also been missed by fitting numerical results for $\omega(l)$,[27] and which modify the predictions for higher-order wetting transitions.[27] The occurrence of these logarithmic terms can be traced back to the fact that only the zeroth and the first moment of the density profiles exist [see Eqs. (2.36) and (2.37)], which enter into a_3 and a_4. The coefficient a_5 would contain $d_{lg}^{(3)}$and $d_{wl}^{(3)}$, which however, do not exist. Instead a term $\sim l^{-5}\ln l$ appears. Nonetheless its corresponding prefactor is well defined and so is the expansion of $\omega(l)$.

The analytic results in Eqs. (2.31)–(2.35) for the effective interface potential allow us to draw conclusions about the properties of wetting transitions close to the critical point T_c of the bulk system. We consider two important cases: critical wetting [$\Delta\mu=0, \tau=(T_w-T)/T_w \to 0$] with a transition temperature T_w close to T_c, i.e., $\hat{t}=(T_c-T_w)/T_c \ll 1$, and complete wetting ($\Delta\mu \to 0, T>T_w$) close to T_c, i.e., $t=(T_c-T)/T_c \ll 1$. With $a_k=\sum_{i\geq 0} a_{k,i}\tau^i$ and $a_{2,0}=0$ Eqs. (2.38) yields

$$l_0(T)=\hat{l}_0\tau^{-1}(1+\tau/\hat{\tau}_c+\cdots) \tag{2.40}$$

with $\hat{l}_0=3a_{3,0}/|2a_{2,1}|$ and $\hat{\tau}_c=|a_{3,1}/a_{3,0}-a_{2,2}/a_{2,1}+8a_{4,0}a_{2,1}/(9a_{3,0}^2)|^{-1}$. Close to T_c the bulk quantities entering the coefficients a_k vary as $\Delta\rho=\kappa_1 t^\beta$ and $\rho_l=\rho_c+\kappa_2 t^\beta$ with positive amplitudes κ_1 and $\kappa_2=\kappa_1/2$. The coefficients a_3 and a_4 depend on $d_{wl}^{(i)}$, which both in the sharp- and soft-kink approximation is a temperature-independent, microscopic length for $i=1$ and the square of it for $i=2$. However, within our approach we find that both quantities display in fact a *singular* temperature dependence close to T_c:

$$d_{wl}^{(i)}(T \to T_c)=-\frac{1}{\rho_c}\bar{\Gamma}_{wl}^{(i)} t^{-(i\nu-\beta)}, \quad i=1,2 \tag{2.41}$$

which follows from the divergence of the zeroth and first moment of the coverage due to critical adsorption (see Ref. 26 and Sec. IX B in Ref. 1): $\Gamma_{wl}^{(i)}=i\int_0^\infty dz\, z^{i-1}[\rho_{wl}(z)-\rho_l]=\bar{\Gamma}_{wl}^{(i)} t^{-(i\nu-\beta)}+\cdots$. Since we study wetting we have $a_2(T_c=T)=0^+$. Thus with Eq. (2.19) and Fig. 1(a) one has $\bar{\Gamma}_{wl}^{(i)}>0$. $\nu=0.64$ is the critical exponent of the correlation length which behaves as $\xi=\xi_0^- t^{-\nu}$. Combining these results we finally obtain, independent from the adopted definition for l_0 (see Appendix A),

$$\hat{l}_0(T=T_w \to T_c)=\bar{\Gamma}_{wl}^{(1)}\kappa_2^{-1}\hat{t}^{\,1-\nu}, \tag{2.42}$$

and

$$\hat{\tau}_c=\left|\frac{\beta+1}{2}-\nu-6\beta\kappa_2\bar{\Gamma}_{wl}^{(2)}(\bar{\Gamma}_{wl}^{(1)})^{-2}\right|^{-1}\hat{t}\,. \tag{2.43}$$

From Eqs. (2.40), (2.42), and (2.43) we can draw the following conclusions: The strength $\hat{l}_0$ of the τ^{-1} divergence for critical wetting vanishes close to T_c $\sim\hat{t}^{\,1-\nu}$. Simultaneously the critical region $\tau<\tau_c$ below T_w, within which the asymptotic behavior $\sim\tau^{-1}$ of the thickness of the wetting film dominates, shrinks $\sim\hat{t}$ due to the vicinity of the critical point. The combination of these formulas yields the restriction $l_0>\hat{l}_0\hat{\tau}_c^{-1}\sim\hat{t}^{-\nu}\sim\xi$. Thus *without an explicit assumption* our results for the interface potential predict that the critical region for a continuous wetting transition shrinks $\sim(T_c-T_w)$ if T_w comes close to T_c. The width of that critical region is determined by the condition $l_0>\xi(T=T_w)$, which is *a posteriori* consistent with our derivation of the effective interface potential [see Eq. (2.27)]. Therefore we conclude that the presence of a critical point impedes the identification of a continuous wetting transition if it happens to occur close to T_c. This

prediction seems to check with recent experimental results for the wetting transition in the cyclohexane-acetonitrile mixture for which $\hat{\tau} \cong 9 \times 10^{-3}$.[29] Although this experiment is concerned with interfacial wetting in a binary liquid mixture and the above results are derived for wetting of a wall by a one-component fluid, our conclusions are nonetheless valid also in this case, because we shall show in Sec. III that the effective interface potential for interfacial wetting exhibits the same features as that for wetting a wall. The authors of the aforementioned experiment measured the contact angle θ, which vanishes in case of critical wetting of a wall according to Ref. 1:

$$\theta = \theta_0 \tau^{3/2} , \tag{2.44}$$

with $\theta_0 = [\frac{8}{27} |a_{2,1}|^3 a_{3,0}^{-2} (\sigma_{gl}(T_w))^{-1}]^{1/2}$. From our above results and with $\sigma_{gl} \sim t^{2\nu}$ We find for $\hat{t} \ll 1$

$$\theta_0(T_w) = \bar{\theta}_0 \hat{t}^{-3/2+\beta} . \tag{2.45}$$

According to Eq. (2.43) the observation of critical wetting is confined to $\tau \lesssim \hat{t}$ which leads to the requirement $\theta < \theta_{\max}$ with $\theta_{\max} = \theta_0 \hat{t}^{3/2} \sim \hat{t}^{\beta} \to 0$. Thus the range of contact angles that can be used to determine the asymptotic thermal singularity of critical wetting shrinks $\sim (T_c - T_w)^{\beta}$ for T_w close to T_c.

Concerning complete wetting close to T_c we obtain, from Eq. (2.39),

$$l_0(T, \Delta\mu) = (u_3 \rho_w - t_3 \rho_c)^{1/3} (\Delta\mu)^{-1/3} \times [1 + (\Delta\mu / \Delta\bar{\mu})^{1/3} + \cdots] , \tag{2.46}$$

with $\Delta\bar{\mu} = 27 (t_3 \bar{\Gamma}_{wl}^{(1)})^{-3} (u_3 \rho_w - t_3 \rho_c)^4 t^{3(\nu-\beta)} \sim t^{0.92}$.

Alternatively, the condition $l_0 > \xi(T, \Delta\mu = 0)$ leads to the more restrictive requirement

$$\Delta\mu < \Delta\mu_c = (u_3 \rho_w - t_3 \rho_c)(\xi_0^-)^{-3} t^{3\nu} \sim t^{1.92} . \tag{2.47}$$

Therefore upon approaching T_c the $(\Delta\mu)^{-1/3}$ law for complete wetting becomes confined to a rapidly decreasing region $\Delta\mu < t^{1.92}$ (see Fig. 4). Outside this region one finds critical adsorption with $l_0 \sim \xi \sim (\Delta\mu)^{-\nu/\Delta} = (\Delta\mu)^{-0.402}$. These considerations show *explicitly* how the tails of the van der Waals interactions, which lead to the $(\Delta\mu)^{-1/3}$ law, become irrelevant upon approaching T_c compared with the critical phenomena, which lead to the more singular $(\Delta\mu)^{-0.402}$ law.

At the end of this subsection we want to compare the above findings with our previous results in Ref. 10. There we determined the effective interface potential by using $\tilde{\rho}(z, l; T) = \Theta(z - d_w) \rho_{lg}(z - l)$ as a trial function [see Eq. (2.23)]. $\tilde{\rho}(z)$ does include the van der Waals tails of the emerging liquid-gas interface but it differs from the trial function $\rho(z)$ in Eq. (2.26): the wall-liquid interface structure is mimicked only by a step function $\Theta(z - d_w)$ with d_w as an input parameter; consequently, in $\tilde{\rho}(z)$ the van der Waals tail on the liquid side of $\rho_{lg}(z)$ extends

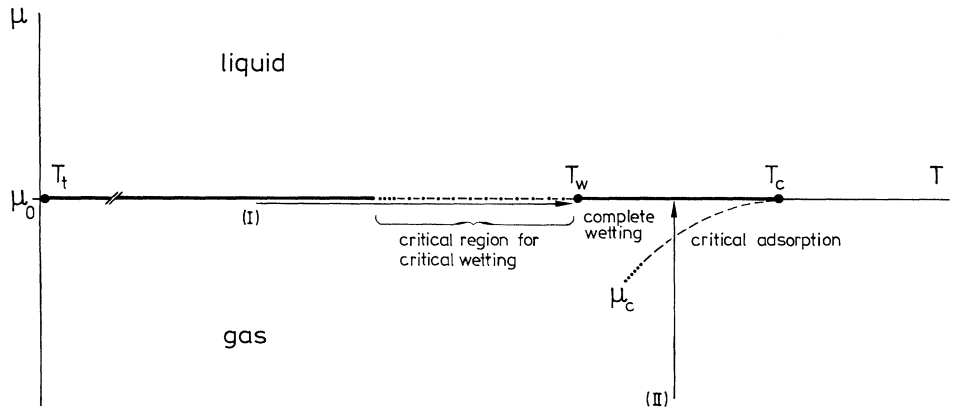

FIG. 4. Schematic drawing of the liquid-gas coexistence curve $\mu_0(T)$ in the bulk phase diagram. For reasons of simplicity it is taken to be a straight line between the triple point T_t and the critical point T_c. T_w is the transition temperature for a critical wetting transition. Along path (I) at μ_0^- the thickness l of the wetting film diverges. Within the critical region for critical wetting this divergence is dominated by the leading power law $l \sim (T_w - T)^{-1}$. The width of this critical region is proportional to $T_c - T_w$. Independent of the order of the wetting transition at T_w l diverges also along the path (II). Within the indicated wedgelike region l diverges $\sim (\Delta\mu)^{-1/3}$ according to complete wetting; $\Delta\mu = \mu_0 - \mu$. Below that region and sufficiently close to T_c l grows $\sim (\Delta\mu)^{-\nu/\Delta}$ with $\nu/\Delta \simeq 0.402$ according to critical adsorption. The crossover between these two power laws occurs at $\mu_c(T) \simeq \mu_0 - \text{const} \times (T_c - T)^{3\nu}$ with $3\nu \simeq 1.92$. For $T \to T_c$ the $(\Delta\mu)^{-1/3}$ law for complete wetting becomes confined to a rapidly decreasing region. This shows explicitly how near T_c universality is restored. This means that the thermal singularities become dominated by bulk critical phenomena which induce the phenomenon of critical adsorption and which lead to stronger singularities than those stemming from the van der Waals interactions, which are irrelevant close to T_c. Both the critical region for critical wetting and $\mu_c(T)$ are determined by the condition $l > \xi$.

down to the wall at $z=d_w$. This ansatz yields[10] an effective interface potential $\tilde{\omega}(l)$ with the identical structure as in Eq. (2.30) but with coefficients $\tilde{a}_k$ where

$$\tilde{a}_2=a_2 ,$$
$$\tilde{a}_3=\tilde{a}_3^{*}+A_3^{(l)}\int_0^{\infty}dz[\rho_l t(z)-\rho_w V(z+d_w)] ,$$
$$\tilde{a}_4=\tilde{a}_4^{*}+\int_0^{\infty}dz[\rho_l t(z)-\rho_w V(z+d_w)] \times[A_4^{(l)}+3(z+d_w)A_3^{(l)}]$$

[see Eqs. (4)–(7) in Ref. 10, and Ref. 30]. The coefficients $\tilde{a}_k^{*}$ are given by the expressions for $\tilde{a}_k$ [Eqs. (2.32) and (2.33)] if in Eqs. (2.34), and (2.35) $d_{wl}^{(1)}$ and $d_{wl}^{(2)}$ are replaced by d_w and $(d_w)^2$, respectively. The appearance of the extra contributions $\sim A_3^{(l)}$ and $\sim A_4^{(l)}$ in $\tilde{a}_3$ and $\tilde{a}_4$ can be traced back to the fact that in the corresponding trial function $\tilde{\rho}(z)$ the van der Waals tail on the liquid side of $\rho_{lg}(z)$ is extending down to $z=d_w$, whereas in the trial function $\rho(z)$ [Eq. (2.26)] this tail reaches only up to $z=\kappa(l)+\lambda(l)\sim\kappa_0 l$. This difference can be understood by using the trial function $\tilde{\rho}(z)$ for the hypothetical problem of the wetting of a compound substrate, which consists of the original substrate particles with density ρ_w for $-\infty\le z\le-\kappa_0 l$ and of the fluid particles with density ρ_l for $-\kappa_0 l<z\le 0$. The substrate potential of this compound is given by $\rho_w\tilde{V}(z)=\rho_w V(z+\kappa_0 l)+\rho_l[t(z)-t(z+\kappa_0 l)]$. If one now applies the formula for the extra contribution to $\tilde{a}_3$ [which belongs to the term $\sim l^{-3}$ in $\tilde{\omega}(l)$] for this compound substrate potential, one obtains $A_3^{(l)}\int_0^{\infty}dz[\rho_l t(z+\kappa_0 l)-\rho_w V(z+\kappa_0 l+d_w)]$, which is proportional to $(\kappa_0 l)^{-2}$ for $l\to\infty$. Similarly, the extra contribution to $\tilde{a}_4$ becomes $\sim(\kappa_0 l)^{-1}$. Therefore in this hypothetical problem these extra terms $\sim A_3^{(l)}$ and $\sim A_4^{(l)}$ do not contribute to the effective interface potential up to and including the order l^{-4} as considered by us. This result checks with the fact that upon using the trial function $\rho(z)$ in Eq. (2.26) these extra van der Waals contributions do not show up in the corresponding coefficients a_k [Eqs. (2.31)–(2.33)], because the application of $\tilde{\rho}(z)$ to this hypothetical problem mimics the application of $\rho(z)$ to the problem of the wetting of the original uniform substrate.

Concerning the properties of wetting transitions close to the critical point T_c the predictions of $\tilde{\omega}(l)$ are[10] that in the case of critical wetting $\hat{t}\to 0$ so that the size of the critical region for the asymptotic power law for continuous wetting shrinks $\sim(T_c-T_w)$. This agrees with our present findings based on $\omega(l)$ [see Eqs. (2.40) and (2.43) and Ref. 31]. However, $\tilde{\omega}$ predicts that the strength of the power law, i.e., $\hat{l}_0$ diverges $\sim\hat{t}^{-1}$ (see Ref. 10), whereas we find now that $\hat{l}_0$ vanishes $\sim\hat{t}^{1-\nu}$ [Eqs. (2.40) and (2.42)]. Also in the case of complete wetting there are differences between the predictions of $\tilde{\omega}(l)$ and $\omega(l)$. For the crossover line $\mu_c(T)$ (see Fig. 4) $\tilde{\omega}(l)$ predicts[10] $\Delta\mu_c\sim t^3$, whereas here we find $\Delta\mu_c\sim t^{3\nu}=t^{1.92}$ [Eq. (2.47)]. These differences are due to the absence of the contributions $\sim A_3^{(l)}$ and $A_3^{(l)}$ (which diverge $\sim t^{-1/2}$ for $T\to T_c$) in the expressions for a_3 and a_4 [see Eqs. (2.32) and (2.33) and the discussion above].

The trial function $\rho(z)$ in Eq. (2.26) is more sophisticated and closer to the exact solution for the density profile than the trial function $\tilde{\rho}(z)$. For this reason the predictions stemming from the effective interface potential $\omega(l)$ seem to be superior to those stemming from $\tilde{\omega}(l)$. In any case this comparison shows how sensitively various wetting properties depend on the precise extension of the van der Waals tails and on the structure of the emerging wall-liquid interface.

E. Deviation of the wall-gas interface profile from superposition

Based on general arguments the actual wall-gas interface profile $\rho_{wg}(z;l)$, including a wetting film of thickness l, exhibits *inter alia* the following limiting properties.

(i) For $l\to\infty$ and z fixed $\rho_{wg}(z;l)$ reduces to the wall-liquid interface profile: $\lim_{l\to\infty}\rho_{wg}(z;l)=\rho_{wl}(z)$.

(ii) For $l\to\infty$ and $z\to\infty$ $\rho_{wg}(z;l)$ reduces to the emerging free liquid-gas interface profile: $\lim_{l\to\infty}\rho_{wg}(z=l+y;l)=\rho_{lg}(y)$.

(iii) For l fixed and $z\to\infty$ $\rho_{wg}(z;l)$ behaves like the wall-gas interface without a wetting film: $\lim_{z\to\infty}[z^3(\rho_{wg}(z;l)-\rho_g)]=Q_3^{(g)}$, independent of l.

The properties (i) and (ii) follow from Antonov's rule and (iii) has been proven in Eqs. (2.20) and (2.21). By using Eqs. (2.11) and (2.23) one can check directly, that the trial function $\rho(z,l;T)$ in Eq. (2.26) does fulfill the requirements (i) and (ii). [Recall that for large l one always has $\kappa(l)+\lambda(l)<l+y$ for any fixed value of y, because $\kappa(l\to\infty)\sim\kappa_0 l$ with $\kappa_0<1$.] However, $\rho(z,l;T)$ does *not* satisfy the requirement (iii). Instead, one has $\lim_{z\to\infty}[z^3(\rho(z;l;T)-\rho_g)]=A_3^{(g)}$, which is independent of the substrate potential [see Eq. (2.25)], whereas $Q_3^{(g)}$ does depend on it [see Eq. (2.21)]. Therefore, for any finite value of l the actual wall-gas density profile cannot be represented only as an appropriate superposition of the wall-liquid and the liquid-gas density profile as is the case for the trial function $\rho(z,l;T)$ in Eq. (2.26).[32] In order to cure this defect we consider an improved trial function $\rho^{*}(z)$:

$$\rho^{*}(z,l;T)=\rho(z,l;T)+\Theta(z-[\kappa(l)-\lambda(l)])\sum_{k\ge 3}D_k z^{-k} , \tag{2.48}$$

with

$$D_3=Q_3^{(g)}-A_3^{(g)}=\rho_g^2(\rho_w u_3-\rho_l t_3)\kappa_T^{(g)} \tag{2.49}$$

and $\rho(z,l;T)$ given by Eq. (2.26); the coefficients D_k are taken to be independent from l. It is straightforward to check that $\rho^{*}(z,l)$ fulfills the requirements (i) and (ii), as $\rho(z,l)$ does, and that, in addition,

$$\rho^{*}(z\to\infty,l;T)=\rho_g+Q_3^{(g)}z^{-3}+Q_4^{(g)}z^{-4}+\cdots \tag{2.50}$$

in accordance with (iii) and with $Q_4^{(g)}=D_4+A_4^{(g)}+3lA_3^{(g)}$. [Note that due to Eq. (A9) one has $A_4^{(g)}+3lA_3^{(g)}=\hat{A}_4^{(g)}+3\hat{l}\,\hat{A}_3^{(g)}$ so that $Q_4^{(g)}$ is indeed independent of the choice of the definition for l.] The

coefficient $Q_3^{(g)}$ in Eq. (2.50) is known [see Eq. (2.21)] and it is independent of l. This dictates our choice for D_3 in Eq. (2.49). The coefficients $Q_k^{(g)}$, $k \geq 4$, which characterize in the limit $z \to \infty$ the (nonequilibrium) wall-gas density profile under the restriction of the presence of a wetting film of thickness l, are unknown; one has to expect that they do depend on this thickness l of a wetting film which is forced to cover the wall. If these coefficients were known they would in turn determine the coefficients D_k (e.g., see the above formula for $Q_4^{(g)}$). In order to be concrete and in the absence of further information we choose $D_k = \rho_g^2(\rho_w u_k - \rho_l t_k)\kappa_l^{(g)}$, $k \geq 4$. However, as it will turn out [cf. Eqs. (2.51)–(2.53)] our final results do not depend on this choice. Thus we restrict our analysis to the case that the coefficients D_k do not depend on increasing powers of l, which in the general case, however, cannot be ruled out.[33]

With a technique which is similar to but even more complicated than the one we used in Sec. II D we were able to obtain analytically the asymptotic behavior $\omega^*(l \to \infty)$ of the effective interface potential corresponding to the trial function $\rho^*(z,l)$ in Eq. (2.48). It has the same structure as $\omega(l)$, which belongs to the trial function $\rho(z,l)$, but with expansion coefficients a_k^* [compare Eqs. (2.30)–(2.35)]:

$$a_2^* = a_2 , \tag{2.51}$$

$$a_3^* = a_3 , \tag{2.52}$$

and

$$a_4^* = a_4 , \tag{2.53}$$

where a_2, a_3, and a_4 are given by Eqs. (2.31)–(2.35).

The striking aspect of these results is that the extra terms $\sim D_k$ in Eq. (2.48) leave all three expansion coefficients a_2^*, a_3^*, and a_4^* unchanged compared with those following from the trial function $\rho(z,l)$. However, we want to emphasize that the reasons leading to Eq. (2.51) and Eqs. (2.52) and (2.53), respectively, differ significantly. Whereas the extra terms $\sim D_k$ do not generate any contribution $\sim l^{-2}$ in the effective interface potential, they do generate an infinite number of terms $\sim l^{-3}$ and $\sim l^{-4}$ which, however, after a lengthy resummation procedure turn out to cancel each other so that $a_3^* = a_3$ and $a_4^* = a_4$. Furthermore, our calculations show that Eqs. (2.51)–(2.53) remain valid for any choice of the coefficients D_k, in particular for $k \geq 4$, as long as they are not increasing functions of l.

Thus we can conclude that these findings enhance considerably our confidence in those results we derived previously [see Eqs. (2.31)–(2.35)]. One may even speculate whether the expressions for the asymptotic behavior of the effective interface potential as given in Eqs. (2.31)–(2.35) are exact. In particular, our discussion of the wetting behavior close to T_c [see Eqs. (2.38)–(2.47)] remains unchanged.

III. INTERFACIAL WETTING IN BINARY LIQUID MIXTURES

For conceptual reasons, in order to study wetting phenomena, it is natural to focus first on the wetting of a wall by a fluid because in this case the boundary, which breaks the translational invariance, is fixed externally and leads to a prescribed substrate potential. However, this conceptual advantage is accompanied by several difficulties both in theory and experiment which are caused by the presence of this wall. None of these difficulties quoted below is addressed by the model in Sec. II. But even the application of more sophisticated density functionals has been hardly successful in solving properly even some of these difficulties. First, as already mentioned in Sec. II, the presence of a hard wall leads to density oscillations in the fluid close to it. The local pressure close to the wall together with the corrugation of the substrate may lead to the formation of one or even more solidlike layers of the adsorbate on the substrate, which in turn are subject to strain effects. Second, the substrate potential itself is a function of temperature and pressure as any solid phase. Third, the adsorption process modifies the substrate potential due to a compression stemming from the adsorbate and due to structural changes of the first few wall layers caused by the adsorbed particles. Fourth, to a certain extent the wall particles may dissolve in the fluid and by interdiffusion fluid particles may penetrate into the solid which altogether leads to a contamination of the system just at the interface of interest. Fifth, defects in the solid wall (which must be there even in thermal equilibrium) as well as surface roughness introduce randomness in the substrate potential.

All these difficulties arise because in reality the wall is not inert but tends towards thermal equilibrium with the adsorbed fluid. In this situation one has basically two options. Either one carefully chooses a wall material, which minimizes these disturbing effects and remains in a restricted thermal equilibrium during the relevant observation time, or one fully includes the wall into the calculation of the thermal equilibrium of the whole coupled wall-fluid system. In the case of a solid as a confining material of the fluid at present this second option is out of reach. If, however, the confining material is a fluid itself, this program can be fully implemented by considering the interface between, say, the A-rich liquid phase and the vapor phase of a binary liquid mixture consisting of A and B particles. In this case one can study the wetting of the intrinsic A-rich-liquid–vapor interface by the B-rich liquid phase. (The experimental and theoretical status of these interfacial wetting phenomena together with the corresponding literature is discussed in Secs. V D and IV C, respectively, in Ref. 1; see also Ref. 14 and the references therein.)

In the analysis of the *interfacial wetting phenomena* at the liquid-vapor interface of binary liquid mixtures all the aforementioned difficulties are no longer present. Instead, new ones arise. First the parameter space is increased. Now there are three interaction potentials, w_{AA}, w_{BB}, and w_{AB}, replacing the substrate potential and the fluid-fluid interaction in the case of a one-component fluid at a wall. Second, the translational invariance is no longer broken explicitly by a wall but more indirectly by imposing boundary conditions: for $z \to -\infty$ there is the A-rich liquid phase, denoted as the α phase, and for $z \to \infty$ there is the vapor phase, denoted as the γ phase.

The wetting phase is the B-rich liquid denoted by β. Third, now there are six relevant bulk number densities ($\rho_{A,\alpha}$, $\rho_{A,\beta}$, $\rho_{A,\gamma}$, $\rho_{B,\alpha}$, $\rho_{B,\beta}$, and $\rho_{B,\gamma}$) and two relevant density profiles $\rho_A(z)$ and $\rho_B(z)$. In Sec. II we had only ρ_l, ρ_g, and $\rho(z)$. Fourth, in order to observe interfacial wetting the system must be kept close to three-phase coexistence along the triple line (see Fig. 5). This requires fixing two of the three relevant thermodynamic variables T, μ_A, and μ_B compared with one out of T and μ in Sec. II. Thus the γ phase is not, e.g., air but the equilibrium vapor phase of the binary liquid mixture. Fifth, the wetting of the α-γ interface leads to the formation of two fluid interfaces, α-β and β-γ, which *both* exhibit capillary fluctuations, whereas in the case of the wetting of a wall there is only one fluctuating interface. However, as in the latter case, it turns out that these interface fluctuations are irrelevant for thermal singularities of the continuous wetting transition because binary liquid mixtures are governed by long-range van der Waals forces (see Refs. 12 and Sec. IV C in Ref. 1). Therefore we can again apply a mean-field-type density-functional theory, cf. Eq. (3.1), which generalizes Eq. (2.1) to the case of a two-component system. One should note that due to the absence of the aforementioned density oscillations at the emerging α-β and β-γ interfaces Eq. (3.1) is even more appropriate for studying the wetting phenomena under consideration than Eq. (2.1) for the case of the wetting of a wall. Sixth, as discussed above the analysis of the wetting of a wall is impeded by the approach of the wall towards thermal equilibrium. For interfacial wetting phenomena one faces the opposite problem. Since the theoretical predictions apply for complete thermal equilibrium, a comparison with experimental data requires a careful equilibration of the experimental system. If the starting configuration in the experiment involves macroscopically thick wetting films it is known that thinning towards their equilibrium thickness may take a very long time.[34] However, this difficulty can be overcome by avoiding in the experimental starting configuration thick wetting films and by studying thin wetting films; their growth towards their thickness in thermal equilibrium is sufficiently fast compared with the experimental observation time (see Sec. XII in Ref. 1). Therefore the theoretical predictions for thermal equilibrium do not evade possible experimental checks.

Thus we can conclude that with respect to a number of aspects the study of interfacial wetting offers several advantages compared with the wetting of a wall. The binary liquid mixtures are more complex than a one-component fluid. However, as discussed above this additional complexity can be brought under control both in theory and experiment. For these reasons in the following subsections we carry through an analytic analysis of interfacial wetting in analogy to what we have done in Sec. II for the wetting of a wall. Our results will improve previous analytic studies of such systems with long-range forces, which were based on the sharp-kink and soft-kink approximation (see Refs. 8 and 9, respectively).

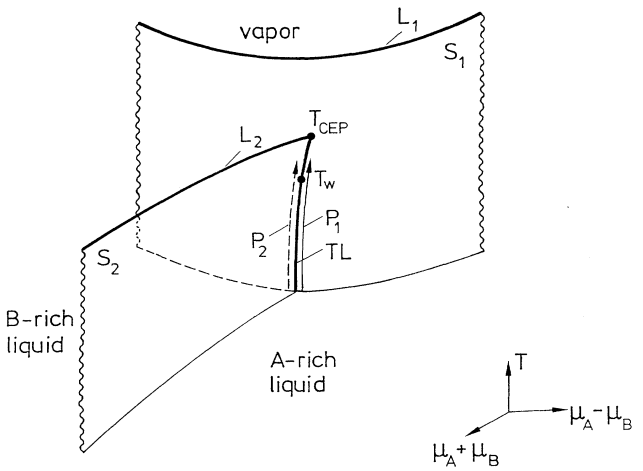

FIG. 5. Bulk phase diagram of a simple binary liquid mixture (type II, see Ref. 14) in the space of temperature T and the chemical potentials μ_A and μ_B of the A and B particles, respectively. The sheet S_1 is the locus of first-order phase transitions separating the liquid phases from the vapor, whereas S_2 separates the A-rich liquid phase from the B-rich liquid phase. S_1 and S_2 are bounded by lines L_1 and L_2 of critical points. The critical end point T_{CEP} is the intersection between L_2 and S_1. The sheets S_1 and S_2 meet at the triple line TL, which ends at T_{CEP}. We are considering interfacial wetting phenomena along the paths p_1 and p_2, respectively, which for reasons of clarity are taken slightly off the triple line, but both lying on S_1. Along p_1 at T_w the B-rich liquid phase wets the A-rich-liquid–vapor interface, whereas along p_2 the A-rich liquid wets the B-rich-liquid–vapor interface. Interfacial wetting occurs either along p_1 or p_2. If TL between T_w and T_{CEP} is approached on S_1 complete wetting occurs. In the case of a first-order wetting transition a prewetting line is attached to T_w, which lies on S_1 and joins TL tangentially. For reasons of clarity we omitted it.

A. Density functional

As stated above we start from the following density functional for inhomogeneous binary liquid mixtures:

$$\Omega[\{\rho_i(\mathbf{r})\};T,\mu_i;\{w_{ij}(|\mathbf{r}-\mathbf{r}'|)\}]=\int d^3r\, f_h(\rho_i(\mathbf{r}),T)+\tfrac{1}{2}\sum_{i,j}\int dr^3\int d^3r'\bar{w}_{ij}(|\mathbf{r}-\mathbf{r}'|)\rho_i(\mathbf{r})\rho_j(\mathbf{r}')$$
$$-\sum_i \mu_i\int d^3r\,\rho_i(\mathbf{r}),\quad i=A,B\ . \tag{3.1}$$

$\Omega[\{\rho_A(\mathbf{r}),\rho_B(\mathbf{r})\};T,\mu_A,\mu_B]$ is the grand canonical potential for a given pair of number density profiles $\rho_A(\mathbf{r})$ and $\rho_B(\mathbf{r})$ for the A and B particles, respectively. The fluid particles interact via spherically symmetric pair potentials $w_{AA}(r)$, $w_{BB}(r)$, and $w_{AB}(r)$, which are attractive at large distances r where they decay $\sim r^{-6}$. In Ref. 14 (where the same notation is used as here) the reader can find the derivation of Eq. (3.1) as well as a detailed discus-

sion of it. It includes the definition of f_h and the connection between the potentials $\{w_{ij}\}$ and the functions $\{\tilde{w}_{ij}\}$ entering Eq. (3.1), which differ only at small distances.

In thermal equilibrium the actual number density profiles $\rho_{i,0}(\mathbf{r};T,\mu_i)$ minimize Eq. (3.1) in accordance with the imposed boundary conditions at $z=\pm\infty$. For a homogeneous bulk system of volume V one has $\Omega=V\Omega_b$ with

$$\Omega_b=f_h(\rho_A,\rho_B,T)+\tfrac{1}{2}\sum_{i,j}w_{0,ij}\rho_i\rho_j-\sum_i\mu_i\rho_i\ , \tag{3.2}$$

where

$$w_{0,ij}=\int_{-\infty}^{\infty}dz\,\hat{w}_{ij}(z)\ , \tag{3.3}$$

with

$$\hat{w}_{ij}(z)=\int d^2r_\parallel\tilde{w}_{ij}[(r_\parallel^2+z^2)^{1/2}]\ . \tag{3.4}$$

In analogy with Eq. (2.7) we define

$$\begin{aligned}t_{ij}(z)&=\int_z^{\infty}dz'\hat{w}_{ij}(z')\\&=-\sum_{k\geq 3}t_{ij,k}z^{-k},\quad z\gg\max(\sigma_A,\sigma_B)\end{aligned} \tag{3.5}$$

so that $w_{0,ij}=2t_{ij}(0)$. σ_i is the hard-core diameter of type-i particles.

If one chooses, e.g., $w_{0,AB}$ as a scale for the temperature T and for the chemical potentials μ_A and μ_B of the A and B particles, respectively, the type of the bulk phase diagram predicted by Eq. (3.2) depends only on three numbers: $w_{0,AA}/w_{0,AB}$, $w_{0,BB}/w_{0,AB}$, and $r=\sigma_A/\sigma_B$.[14] All the various bulk phase diagrams predicted by Eq. (3.2) allow for the formation of (at least) three phases: a vapor phase (γ) and two liquid phases, one rich in A particles and the other rich in B particles.[14] Figure 5 shows one representative of such bulk phase digrams (a so-called type-II phase diagram). Our following analysis is confined to the vicinity of the triple line, where all three fluid phases coexist and along which interfacial wetting occurs. However, we want to underscore that the formulas in Secs. III B and III C are *generally* valid and applicable to *all* types of bulk phase diagrams predicted by Eq. (3.2).

B. Structure of the fluid-fluid interfaces

Let us consider such values of T, μ_A, and μ_B for which in the bulk the binary liquid mixture is at two-phase coexistence between two fluid phases κ and ν, i.e., the system is located on one of the two coexistence sheets shown in Fig. 5: $(\kappa,\nu)=(\alpha,\beta)$, (β,γ), or (α,γ). This allows us to impose the boundary conditions $\rho_i(z\to-\infty)=\rho_{i,\kappa}$ and $\rho_i(z\to+\infty)=\rho_{i,\nu}$, $i=A,B$, so that a κ-ν interface is formed whose position we denote by $z=0$. (Concerning the choice for the position of this free interface the same arguments apply as in Sec. II C and in Appendix A for the liquid-gas interface in a one-component fluid.) For this configuration Eq. (3.1) splits into a bulk and into a surface contribution: $\Omega=V(\Omega_{b,\kappa}+\Omega_{b,\nu})/2+A\,\Omega_s^{(\kappa,\nu)}$. For Ω_s one obtains with $\rho_i(\mathbf{r})=\rho_i(z)$

$$\begin{aligned}\Omega_s^{(\kappa,\nu)}[\{\rho_i(z)\};T,\mu_i;\{w_{ij}(r)\}]=&\int_{-\infty}^{\infty}dz[f_h(\rho_i(z),T)-f_h(\rho_{i;\kappa,\nu}^{shk}(z),T)]\\&+\tfrac{1}{2}\sum_{i,j}\int_{-\infty}^{\infty}dz\int_{-\infty}^{\infty}dz'\hat{w}_{ij}(|z-z'|)\delta\rho_{i;\kappa,\nu}(z)\delta\rho_{j;\kappa,\nu}(z')\\&+\sum_i\int_{-\infty}^{\infty}dz\left[\left[\sum_j w_{0,ij}\rho_{j;\kappa,\nu}^{shk}(z)\right]-\mu_{0,i}^{(\kappa,\nu)}\right]\delta\rho_{i;\kappa,\nu}(z)\\&+\sum_i(\rho_{i,\kappa}-\rho_{i,\nu})\sum_j\int_{-\infty}^{\infty}dz[\mathrm{sgn}(z)]t_{ij}(|z|)\delta\rho_{j;\kappa,\nu}(z)\\&-\tfrac{1}{2}\sum_{i,j}(\rho_{i,\kappa}-\rho_{i,\nu})(\rho_{j,\kappa}-\rho_{j,\nu})\int_0^{\infty}dz\,t_{ij}(z)\ ,\end{aligned} \tag{3.6}$$

with $\delta\rho_{i;\kappa,\nu}(z)=\rho_i(z)-\rho_{i;\kappa,\nu}^{shk}(z)$; $\rho_{i;\kappa,\nu}^{shk}(z)=\Theta(z)\rho_{i,\nu}+\Theta(-z)\rho_{i,\kappa}$ is the sharp-kink approximation for the number density profile of the particles of type i for the free κ-ν interface. $\mu_{0,i}^{(\kappa,\nu)}$ denotes those values of the chemical potentials for which at a given temperature T the two bulk phases κ and ν coexist. At these values of T and μ_i $\rho_{A,\kappa}$, $\rho_{B,\kappa}$, $\rho_{A,\nu}$, and $\rho_{B,\nu}$ are the corresponding bulk number densities in thermal equilibrium. (Here we dropped the additional index 0 denoting equilibrium values.) Equation (3.6) is valid for any pair of trial functions $\rho_i(z)$, which for $z\to\pm\infty$ approach their limiting values $\rho_{i,\kappa}$ and $\rho_{i,\nu}$, respectively, rapidly enough so that the integrals in Eq. (3.6) do exist. If the A and B particles are identical Eq. (3.6) reduces to Eq. (2.22). The actual pair of κ-ν interface profiles $\rho_{i;\kappa,\nu}[z;T,\mu_{0,i}^{(\kappa,\nu)};\{w_{ij}\}]$ minimizes Eq. (3.6) and renders the κ-ν surface tension $\sigma_{\kappa\nu}[T,\mu_{0,i}^{(\kappa,\nu)};\{w(r)\}]$. As in the one-component case one has, for any z_0, $\Omega_s^{(\kappa,\nu)}[\{\rho_i(z)\}]=\Omega_s^{(\kappa,\nu)}[\{\rho_i(z+z_0)\}]$ so that the position of the free κ-ν interface is not fixed. Qualitatively $\rho_{i;\kappa,\nu}(z)$ looks similar to $\rho_{lg}(z)$ in Fig. 1(b), i.e., there is a main transition region around its center, taken to be at $z=0$, with width $2\xi_i$ and van der Waals tails on the κ and ν side, i.e., for $z\to-\infty$ and $z\to+\infty$, respectively. The form of these density profiles is not known analytically. Therefore we write in analogy with Eq. (2.23) ($i=A,B$):

$$\rho_{i;\kappa,\nu}(z)=\begin{cases}\rho_{i,\kappa}-\sum_{k\geq 3}A_{i,k}^{(\kappa;\kappa,\nu)}|z|^{-k}, & z\leq-\xi_i\\ F_i^{(\kappa,\nu)}(z), & |z|\leq\xi_i\\ \rho_{i,\nu}+\sum_{k\geq 3}A_{i,k}^{(\nu;\kappa,\nu)}z^{-k}, & z\geq\xi_i\ .\end{cases} \tag{3.7}$$

Thus any κ-ν interface is described by two correlation lengths ξ_i, two smooth functions $F_i(z)$ around the center of the interface, and four van der Waals tails. $\rho_{i;\kappa,\nu}(z)$ minimize Eq. (3.6) and they are solutions of the following system of integral equations ($i,j=A,B$):

$$\mu_{i,0}^{(\kappa,\nu)}=\frac{\partial f_h}{\partial \rho_i}[\rho_{i;\kappa,\nu}(z),T] + \sum_j \int_{-\infty}^{\infty} dz' \hat{w}_{ij}(|z-z'|)\rho_{j;\kappa,\nu}(z') \ . \tag{3.8}$$

Equation (3.8) can be analyzed along the same lines as Eq. (2.23) yielding the four coefficients $A_{i,3}^{(\kappa;\kappa,\nu)}$ and $A_{i,3}^{(\nu;\kappa,\nu)}$ which determine the leading asymptotic behavior of $\rho_{i;\kappa,\nu}(z)$ for $|z|\to\infty$ [see Eq. (3.7)]. After a lengthy calculation one obtains

$$A_{i,3}^{(\lambda;\kappa,\nu)}=\frac{\rho_\lambda^2}{\det(1/\kappa_{ij}^{(\lambda)})} \times \sum_j (\rho_{j,\kappa}-\rho_{j,\nu}) \left[\frac{t_{ij,3}}{\kappa_{C_iC_i}^{(\lambda)}} - \frac{t_{C_ij,3}}{\kappa_{AB}^{(\lambda)}} \right] , \tag{3.9}$$

with $i,j=A,B$; $\lambda=\kappa,\nu$; $C_A=B$ and $C_B=A$; and $\rho_\lambda=\rho_{A,\lambda}+\rho_{B,\lambda}$. Denoting N_i as the number of particles of type i within the volume V the partial isothermal compressibilities are defined as

$$\kappa_{ij}=\frac{V}{N^2}\left[\frac{\partial N_i}{\partial \mu_j}\right]_{T,V} =\rho^{-2}\left[\frac{\partial \rho_i}{\partial \mu_j}\right]_{T,V} =\rho^{-2}\left[\frac{\partial^2 f_h}{\partial\rho_i\partial\rho_j}+w_{0,ij}\right]^{-1} ; \tag{3.10}$$

$\kappa_{ij}^{(\lambda)}$ is obtained by evaluating the last equation of Eq. (3.10) at $\rho_i=\rho_{i,\lambda}$ and $\rho=\rho_\lambda$. Note that $A_{i,3}^{(\lambda;\kappa,\nu)}$ are dimensionless quantities. To the best of our knowledge Eq. (3.9) has not yet been derived previously. As in the one-component case the higher-order coefficients $A_{i,k}^{(\lambda;\kappa,\nu)}$, $k\geq 4$, depend on the choice for the position of the free interface.

C. Effective interface potential for interfacial wetting

If a system, like a binary liquid mixture, exhibits the possibility of three-phase coexistence involving the distinct phases α, β, and γ, the three different interfaces α-β, α-γ, and β-γ can be formed. The application of Antonov's rule to these three interfaces shows that, if one of them undergoes an interfacial wetting transition, none of the other two can be wet, too. Therefore without loss of generality we can focus on the case that the α-γ interface may be wetted by the β phase and that neither the α-β interface is wetted by the γ phase nor the β-γ interface is wetted by the α phase. One can associate the γ phase with the vapor phase, the α phase with A-rich liquid phase, and the β phase with the B-rich liquid phase. With this identification one is studying the wetting transition at the liquid-vapor interface. However, as already pointed out, the following considerations are independent of such an identification.

Following the spirit of Sec. II D we want to determine the asymptotic behavior of the effective interface potential $\Omega_s^{(\alpha,\gamma)}(l)$ for the formation of a β-like layer of thickness l at the α-γ interface. In the process of a continuous wetting transition the free α-β and β-γ interfaces emerge smoothly out of the α-γ interface. In analogy to Sec. II D we calculate $\Omega_s^{(\alpha,\gamma)}(l)=\sigma_{\alpha\beta}+\sigma_{\beta\gamma}+\omega_{\alpha\gamma}(l)$ by evaluating Eq. (3.6) for a pair of trial functions $\rho_i(z,l;T)$, which are suitable superpositions of the density profiles at the (necessarily nonwet) α-β and β-γ interfaces. $\sigma_{\alpha\beta}$ and $\sigma_{\beta\gamma}$ are the minimum values of $\Omega_s^{(\alpha,\beta)}$ and $\Omega_s^{(\beta,\gamma)}$, respectively, and $\sigma_{\alpha\gamma}=\min_l \Omega_s^{(\alpha,\gamma)}(l)$ is the minimum value of $\Omega_s^{(\alpha,\gamma)}$ in Eq. (3.6). As a generalization of Eq. (2.26) we make the following choice for these trial functions ($i=A,B$):

$$\rho_i(z,l;T)=\begin{cases} \rho_{i;\alpha,\beta}(z), & z\leq\kappa(l)-\lambda(l) \\ G_i(\kappa(l)-z,l), & \kappa(l)-\lambda(l)\leq z\leq\kappa(l)+\lambda(l) \\ \rho_{i;\beta,\gamma}(z-l), & z\geq\kappa(l)+\lambda(l) \ . \end{cases} \tag{3.11}$$

Thus the trial function consists of the density profiles of the free α-β interface [Eq. (3.7)] centered around $z=0$ and of those of the free β-γ interface [Eq. (3.37)] centered around $z=l$. The pair of functions G_i describes the smooth crossover between them in the transition region around $z=\kappa(l)$. $\rho_i(z,l;T)$ exhibits a similar structure as $\rho(z,l)$ in Fig. 3 provided that there $\rho_{wl}(z)$ is replaced by $\rho_{i;\alpha,\beta}(z)$, which extends to $z=-\infty$. For the functions $G_i(z,l)$, $\kappa(l)$, and $\lambda(l)$ we impose the same restrictions as for the analogous ones appearing in Eq. (2.26). Note that we use the same thickness l for both density profiles $\rho_A(z)$ and $\rho_B(z)$.

In Eq. (3.11) $\rho_i(z,l;T)$ is defined only along the triple line $\tilde{\mu}_i(T)$. In order to be able to study also complete interfacial wetting Eq. (3.11) must be generalized to the case that the system is still at α-γ coexistence, i.e., $\mu_i=\mu_{0,i}^{(\alpha,\gamma)}$ but off the triple line. As the simplest generalization we choose

$$\rho_i(z,l;T,\mu_{0,i}^{(\alpha,\gamma)})=\rho_i(z,l;T)+\Theta(z-l)[\rho_{i,\gamma}(T,\mu_{0,i}^{(\alpha,\gamma)})-\rho_{i,\gamma}(T,\tilde{\mu}_i(T))]+\Theta(-z)[\rho_{i,\alpha}(T,\mu_{0,i}^{(\alpha,\gamma)})-\rho_{i,\alpha}(T,\tilde{\mu}_i(T))] \ . \tag{3.12}$$

After a slight generalization the discussion following Eq. (2.28) applies also to Eq. (3.12). In particular, Eq. (3.12) means that even off the triple line $\rho_{i,\beta}$, which enters Eq. (3.12) via Eqs. (3.7) and (3.11), is taken to be the value of the bulk den-

sity ρ_i of the β phase *at* the triple line.

With a technique similar to the one we used in Sec. II D we have been able to determine the asymptotic behavior of the effective interface potential for $l\to\infty$ which follows after inserting Eqs. (3.7) (3.11) and (3.12) into Eq. (3.6) for $(\kappa,\nu)=(\alpha,\gamma)$. We would like to note that, although already the corresponding calculations for a one-component fluid wetting a wall have been extremely tedious, the analytic analysis in the case of interfacial wetting in binary liquid mixtures becomes substantially more difficult: *inter alia*, here we must deal with eight different van der Waals tails compared with three in the one-component case. Therefore we only quote our final results for the effective interface potential $\omega_{\alpha\gamma}(l)=\Omega_s^{(\alpha,\gamma)}(l)-\sigma_{\alpha\beta}-\sigma_{\beta\gamma}$:

$$\omega_{\alpha\gamma}(l)=\sum_i(\tilde{\mu}_i-\mu_{0,i}^{(\alpha,\gamma)})\{[\rho_{i,\beta}-\tfrac{1}{2}(\rho_{i,\alpha}+\rho_{i,\gamma})](l+d_{i,\beta\gamma}^{(1)}-d_{i,\alpha\beta}^{(1)})+\tfrac{1}{2}(\rho_{i,\alpha}-\rho_{i,\gamma})(d_{i,\alpha\beta}^{(1)}+d_{i,\beta\gamma}^{(1)})\}+\sum_{k=2}^{4}a_k l^{-k}+O(l^{-5}\ln l)\ , \tag{3.13}$$

with $(i,j=A,B)$

$$a_2=a_2^{(0)}\ , \tag{3.14}$$

$$a_3=a_3^{(0)}+\sum_{i,j}T_{ij,3}(d_{i,\alpha\beta}^{(1)}-d_{j,\beta\gamma}^{(1)})\ , \tag{3.15}$$

and

$$a_4=a_4^{(0)}+\sum_{i,j}[\tfrac{3}{2}T_{ij,3}(d_{i,\alpha\beta}^{(2)}+d_{j,\beta\gamma}^{(2)}-2d_{i,\alpha\beta}^{(1)}d_{j,\beta\gamma}^{(1)})+T_{ij,4}(d_{i,\alpha\beta}^{(1)}-d_{j,\beta\gamma}^{(1)})]\ , \tag{3.16}$$

where

$$a_k^{(0)}=\frac{1}{k}\sum_{i,j}T_{ij,k+1} \tag{3.17}$$

are the expressions for these coefficients as obtained within the sharp-kink approximation.[8] In order to present these results in the compact form of Eqs. (3.14)–(3.17) we have introduced the following abbreviations:

$$T_{ij,k}=(\rho_{i,\alpha}-\rho_{i,\beta})(\rho_{j,\beta}-\rho_{j,\gamma})t_{ij,k} \tag{3.18}$$

and [compare Eqs. (2.36) and (2.37)]

$$d_{i,\kappa\nu}^{(n)}=\frac{n}{\rho_{i,\kappa}-\rho_{i,\nu}}\int_{-\infty}^{\infty}dz\,z^{n-1}\delta\rho_{i;\kappa,\nu}(z)\ , \tag{3.19}$$

where $n=1,2$; $i=A,B$; and $(\kappa,\nu)=(\alpha,\beta),(\beta,\gamma)$.

As in Eq. (2.30) the explicit form of the first term in Eq. (3.13), which describes complete wetting, is correct up to first order in $\tilde{\mu}_i-\mu_{0,i}^{(\alpha,\gamma)}$. We omitted again the lengthy terms which are nonlinear in $\tilde{\mu}_i-\mu_{0,i}^{(\alpha,\gamma)}$ and which are also linear in l. Therefore in this first term in Eq. (3.13) $\rho_{i,\alpha}$, $\rho_{i,\gamma}$, $d_{i,\alpha\beta}^{(1)}$, and $d_{i,\beta\gamma}^{(1)}$ are taken at coexistence $\mu_i=\tilde{\mu}_i$. By construction $\rho_{i,\beta}$ is always evaluated at $\mu_i=\tilde{\mu}_i$. In deriving this first term in Eq. (3.13) we used the fact that on the triple line both $\rho_{i,\alpha\beta}(z)$ and $\rho_{i,\beta\gamma}(z)$, which enter the trial function in Eq. (3.12), fulfill Eq. (3.8).

The dependence of the coefficients a_k on μ_i turns out to be analogous to that in the one-component case. In their common prefactor $(\rho_{i,\alpha}-\rho_{i,\beta})(\rho_{j,\beta}-\rho_{j,\gamma})$ both $\rho_{i,\alpha}$ and $\rho_{i,\gamma}$ are taken at their actual value at α-γ coexistence but off the triple line, whereas $\rho_{i,\beta}$ is taken at the triple line by construction. It turns out that all the other quantities $d_{i,\kappa\nu}^{(n)}$ have to be taken at the triple line $\tilde{\mu}_i$. These rules hold for arbitrary values of μ_i and not only up to first order in $\tilde{\mu}_i-\mu_{0,i}^{(\alpha,\gamma)}$.

Before we start to discuss these results we want to make two remarks. First, in the appropriate limit Eqs. (3.14)–(3.16) reduce to the results obtained previously within the soft-kink approximation [see Eqs. (3.9)–(3.12) in Ref. 9, and Ref. 35]. Note that in that version of the soft-kink approximation, which has been applied in Ref. 9 for the case of binary liquid mixtures, the density profiles have been taken to vary linearly around their centers. For such profiles $d_{i,\alpha\beta}^{(1)}=0=d_{j,\beta\gamma}^{(1)}$ so that in this case $a_3=a_3^{(0)}$ in accordance with Eq. (3.10) in Ref. 9. However, as Eq. (3.15) shows one has $a_3\neq a_3^{(0)}$ and the difference is determined by the symmetric part of the free interface profiles around their center. In addition, our present approach predicts terms $\sim l^{-5}\ln l$ [see Eq. (3.13)] which are missed both by the sharp- and soft-kink approximation (see Refs. 8 and 9). Second, also in the appropriate limit Eqs. (3.13)–(3.19) reduce to the results for wetting of a wall by a one-component fluid [see Eqs. (2.30)–(2.37)]. In order to achieve this reduction one has to make the following identifications; α denotes wall, β denotes liquid, γ denotes gas, $\rho_{A,\alpha}=\rho_w$, $\rho_{A,\beta}=\rho_{A,\gamma}=\rho_{B,\alpha}=0$, $\rho_{B,\beta}=\rho_l$, $\rho_{B,\gamma}=\rho_g$, $t_{AA}(z)\equiv 0$, $t_{AB}(z)=V(z)$, $t_{BB}(z)=t(z)$, and $G_A(z)\equiv 0$. In addition, the expressions for $\rho_{i;\kappa,\nu}(z)$ must be identified properly. Note that—as it must be in the grand canonical ensemble—Eq. (3.13) displays explicitly the obvious symmetry $\omega_{\alpha\gamma}(l)=\omega_{\gamma\alpha}(l)$. Furthermore, by exploiting the Clausius-Clapeyron equation for binary liquid mixtures at the α-γ coexistence line for constant T (see Fig. 5) one finds that the coefficient multiplying l in Eq. (3.13) vanishes $\sim(T_{\rm CEP}-T)^{\beta}$ for $T\to T_{\rm CEP}$.

As discussed in detail in Appendix A the values of $d_{i,\kappa\nu}^{(n)}$ depend on the definition of what we call the thickness l of the wetting film. Accordingly one obtains different

effective interface potentials; however, such quantities like the value of T_w and the locus of the separatrix between first- and second-order interfacial wetting transitions must be independent of these different possible definitions of l. In the case of wetting of a wall by a one-component fluid the thickness l is fixed by selecting a certain point z^* of the wall-gas interface profile, e.g., by requiring $\rho_{wg}(z=z^*)=(\rho_l+\rho_g)/2$. Then we have $z^*=l$, which also fixes the value of $d_{lg}^{(1)}$ according to our construction scheme of the effective interface potential. $d_{lg}^{(1)}$ is the only quantity which reflects and proliferates a specific choice of definition for l. Once $d_{lg}^{(1)}$ has been fixed this way, $d_{lg}^{(2)}$ is uniquely determined [see Eq. (2.37)]. The presence of the wall fixes the coordinate $z=0$ so that l can be naturally defined by selecting a *single* point z^* based on a certain requirement for a *single* density profile. However, in the case of interfacial wetting in binary liquid mixtures the definition of l requires the selection of *two* points, $z_{\alpha\beta}^*$ and $z_{\beta\gamma}^*$, where each of them is a characteristic point of the emerging α-β and β-γ interface, respectively, which are both described by *pairs* of density profiles, $\rho_A(z)$ and $\rho_B(z)$. As an example, if $\rho_{A;\alpha,\gamma}(z=z_{\alpha\beta}^A)=(\rho_{A,\alpha}+\rho_{A,\beta})/2$ and $\rho_{B;\alpha,\beta}(z=z_{\alpha\beta}^B)=(\rho_{B,\alpha}+\rho_{B,\beta})/2$, one can define $z_{\alpha\beta}^*$ as $z_{\alpha\beta}^{*,\mathrm{I}}=(z_{\alpha\beta}^A+z_{\alpha\beta}^B)/2$. The analogous procedure on the side of the emerging β-γ interface of the wetting film leads to a point $z_{\beta\gamma}^{*,\mathrm{I}}=(z_{\beta\gamma}^A+z_{\beta\gamma}^B)/2$ so that according to this definition $l_{\mathrm{I}}=z_{\beta\gamma}^{*,\mathrm{I}}-z_{\alpha\beta}^{*,\mathrm{I}}$. Other possibilities consist in choosing $z_{\alpha\beta}^{*,\mathrm{II}}=z_{\alpha\beta}^A$ and $z_{\beta\gamma}^{*,\mathrm{II}}=z_{\beta\gamma}^A$, so that $l_{\mathrm{II}}=z_{\beta\gamma}^{*,\mathrm{II}}-z_{\alpha\beta}^{*,\mathrm{II}}$, or $z_{\alpha\beta}^{*,\mathrm{III}}=z_{\alpha\beta}^B$ and $z_{\beta\gamma}^{*,\mathrm{III}}=z_{\beta\gamma}^B$ leading to l_{III}. One can also choose mixed definitions like, e.g., $l_{\mathrm{IV}}=z_{\beta\gamma}^{*,\mathrm{II}}-z_{\alpha\beta}^{*,\mathrm{III}}$. There is an arbitrarily large number of possible definitions. It is helpful to keep in mind that $\rho_{A;\alpha,\gamma}(z)$ and $\rho_{b;\alpha,\gamma}(z)$ represent a pair of solutions to the system of coupled integral equations in Eq. (3.8), so that the *relative* positions of the A-density profiles and B-density profiles are always fixed. Thus each definition $\nu=\mathrm{I},\mathrm{II},\ldots$ for l depends on a pair of definitions (ν_1,ν_2) for selecting $z_{\alpha\beta}^*$ and $z_{\beta\gamma}^*$, respectively. According to our construction scheme for the effective interface potential [see Eq. (3.11)] these definitions fix the values of $d_{A,\alpha\beta}^{(1)}$, $d_{B,\alpha\beta}^{(1)}$, $d_{A,\beta\gamma}^{(1)}$ and $d_{B,\beta\gamma}^{(1)}$ and (therewith also those of $d_{i,\alpha\beta}^{(2)}$ and $d_{i,\beta\gamma}^{(2)}$). According to our above remark about the relative positions of the density profiles only two of the above quantities are independent: $(d_{A,\alpha\beta}^{(1),\nu_1}, d_{A,\beta\gamma}^{(1),\nu_2})$, $(d_{B,\alpha\beta}^{(1),\nu_1}, d_{B,\beta\gamma}^{(1),\nu_2})$, $(d_{A,\alpha\beta}^{(1),\nu_1}, d_{B,\beta\gamma}^{(1),\nu_2})$, or $(d_{B,\alpha\beta}^{(1),\nu_1}, d_{A,\beta\gamma}^{(1),\nu_2})$ parametrizes one and the same definition (ν_1,ν_2); in each case the other two corresponding quantities are fixed. Within our approach for calculating the effective interface potential the change from a definition μ to a definition ν has the following implications $[i=A,B;(\kappa,\lambda)=(\alpha,\beta),(\beta,\gamma)]$:

$$z_{\kappa\lambda}^{*,\nu_a}=z_{\kappa\lambda}^{*,\mu_a}+\Delta z_{\kappa\lambda}\ , \tag{3.20}$$

$$l_\nu=l_\mu-\Delta z_{\alpha\beta}+\Delta z_{\beta\gamma}\ , \tag{3.21}$$

$$d_{i,\kappa\lambda}^{(1),\nu_a}=d_{i,\kappa\lambda}^{(1),\mu_a}-\Delta z_{\kappa\lambda}\ , \tag{3.22}$$

and

$$d_{i,\kappa\lambda}^{(2),\nu_a}=d_{i,\kappa\lambda}^{(2),\mu_a}-2\Delta z_{\kappa\lambda}d_{i,\kappa\lambda}^{(1),\mu_a}+(\Delta z_{\kappa\lambda})^2\ , \tag{3.23}$$

where $a=1$ for $(\kappa,\lambda)=(\alpha,\beta)$ and $a=2$ for $(\kappa,\lambda)=(\beta,\gamma)$. Since the surface free energy of a given density configuration $\rho_{i;\alpha,\gamma}(z)$ does not depend on how the thickness of its wetting layer is defined, one must have $\omega_\nu(l_\nu)=\omega_\mu(l_\mu)$ or $\omega_\nu(l)=\omega_\mu(l+\Delta z_{\alpha\beta}-\Delta z_{\beta\gamma})$. By using Eqs. (3.20)–(3.23) it is straightforward to check that Eqs. (3.13)–(3.19) fulfill this requirement. This represents a highly nontrivial check for the validity of our formulas.

In analogy to Eqs. (A1) and (A2) we are able to cast $\omega_\nu(l)$ in such a form that its dependence on ν becomes explicit, leaving one with a definition-independent potential $\hat{\omega}(l)$. With $\hat{l}_\nu=l+d_{A,\beta\gamma}^{(1),\nu_2}-d_{A,\alpha\beta}^{(1),\nu_1}$ one has at the triple line $\omega_\nu(l)=\hat{\omega}(l=\hat{l}_\nu)$, with $\hat{\omega}(l)$ independent of ν, where

$$\hat{\omega}(l)=\sum_{k=2}^{4}\hat{a}_k l^{-k}+O(l^{-5}\ln l)\ , \tag{3.24}$$

with $\hat{a}_2=a_2$,

$$\hat{a}_3=a_3^{(0)}+\sum_{i,j}T_{ij,3}\hat{\Delta}_{ij}\ , \tag{3.25}$$

and

$$\hat{a}_3=a_4^{(0)}+\tfrac{3}{2}\sum_{i,j}T_{ij,3}\hat{\Gamma}_{ij}+\sum_{i,j}T_{ij,4}\hat{\Delta}_{ij}\ . \tag{3.26}$$

The advantage of representing $\omega(l)$ in terms of $\hat{\omega}(l)$ is that Eqs. (3.24)–(3.26) show explicitly how the effective interface potentials depends on invariant (i.e., independent of ν) lengths $\hat{\Delta}_{ij}$ and products of lengths $\hat{\Gamma}_{ij}$, which are inherent properties of the *free* α-β and β-γ interface profiles. We find

$$\hat{\Delta}=\begin{bmatrix}0 & -\delta_{\beta\gamma,1}\\ \delta_{\alpha\beta,1} & \delta_{\alpha\beta,1}-\delta_{\beta\gamma,1}\end{bmatrix} \tag{3.27}$$

and

$$\hat{\Gamma}=\begin{bmatrix}\delta_{\alpha\beta,2}+\delta_{\beta\gamma,2} & \delta_{\alpha\beta,2}+\delta_{\beta\gamma,3}\\ \delta_{\alpha\beta,3}+\delta_{\beta\gamma,2} & \delta_{\alpha\beta,3}+\delta_{\beta\gamma,3}-2\delta_{\alpha\beta,1}\delta_{\beta\gamma,1}\end{bmatrix}\ , \tag{3.28}$$

where $(\kappa,\lambda)=(\alpha,\beta),(\beta,\gamma)$

$$\delta_{\kappa\lambda,1}=d_{B,\kappa\lambda}^{(1)}-d_{A,\kappa\lambda}^{(1)}\ , \tag{3.29}$$

$$\delta_{\kappa\lambda,2}=d_{A,\kappa\lambda}^{(2)}-(d_{A,\kappa\lambda}^{(1)})^2\ , \tag{3.30}$$

and

$$\delta_{\kappa\lambda,3}=d_{B,\kappa\lambda}^{(2)}+(d_{A,\kappa\lambda}^{(1)})^2-2d_{A,\kappa\lambda}^{(1)}d_{B,\kappa\lambda}^{(1)}\ . \tag{3.31}$$

By using Eqs. (3.22) and (3.23) one can easily check that $\delta_{\kappa\lambda,1}$, $\delta_{\kappa\lambda,2}$, and $\delta_{\kappa\lambda,3}$ are indeed independent from ν. Thus the asymptotic behavior of the effective interface potential for large l is controlled by the matrices T_k [see Eqs. (3.5) and (3.18)], $\hat{\Delta}$ and $\hat{\Gamma}$. The matrix elements of $\hat{\Delta}$ and $\hat{\Gamma}$ are determined by invariant, i.e., intrinsic zeroth and first, respectively, moments of the free α-β and β-γ interface profiles [see Eqs. (3.19) and (3.29)–(3.31)].

According to our remark before Eq. (3.20) there are basically four possibilities for parametrizing the effec-

tive interface potential. For example, with $\tilde{l}_\nu = l + d_{B,\beta\gamma}^{(1),\nu_2} - d_{B,\alpha\beta}^{(1),\nu_1}$ one obtains $\omega_\nu(l) = \tilde{\omega}(l = \tilde{l}_\nu)$ where $\tilde{\omega}(l) = \tilde{a}_2 l^{-2} + \tilde{a}_3 l^{-3} + \tilde{a}_4 l^{-4} + O(l^{-5}\ln l)$ with $\tilde{a}_2 = \hat{a}_2$, $\tilde{a}_3 = a_3^{(0)} + \sum_{i,j} T_{ij,3}\tilde{\Delta}_{i,j}$, etc.,

$$\tilde{\Delta} = \begin{bmatrix} \delta_{\beta\gamma,1} - \delta_{\alpha\beta,1} & -\delta_{\alpha\beta,1} \\ \delta_{\beta\gamma,1} & 0 \end{bmatrix} . \tag{3.32}$$

With Eqs. (3.27) and (3.32) one finds $\tilde{a}_3 = \hat{a}_3 - 2\hat{\Delta}_{BB}\hat{a}_2$. This shows explicitly that although $\tilde{\omega}(l) \neq \hat{\omega}(l)$ both functions render the *same* predictions concerning the physical properties of the system: $\hat{a}_2(T = T_w) = 0 = \tilde{a}_2(T = T_w)$, $\hat{a}_3(T_w) = \tilde{a}_3(T_w)$; similarly, $\hat{a}_4(T_w) = \tilde{a}_4(T_w)$ if $\hat{a}_3(T_w)$ happens to vanish for certain interaction parameters. Thus, as it must be, the value of T_w, which is the wetting transition temperature in case of critical wetting, the separatrix between first and second-order wetting, which is defined by $\hat{a}_3(T_w) = 0$, as well as the separatrix between second- and third-order wetting, which is defined by $\hat{a}_3(T_w) = \hat{a}_4(T_w) = 0$, are determined uniquely.

Finally we want to discuss briefly the complete wetting term in our expression Eq. (3.13) for the effective interface potential. This term can be written as

$$\sum_i (\tilde{\mu}_i - \mu_{0,i}^{(\alpha,\gamma)})[(\rho_{i,\beta} - \rho_{i,\gamma})\hat{l}_\nu + (\rho_{i,\alpha} - \rho_{i,\gamma})d_{i,\alpha\beta}^{(1),\nu_1}] .$$

Whereas the l-dependent piece of this expression is explicitly invariant, there is a constant term—with respect to l—which vanishes $\sim \tilde{\mu}_i - \mu_{0,i}^{(\alpha,\gamma)}$ upon approaching the triple line but which depends on our choice for defining the effective interface potential. In the one-component case this feature does not show up in the corresponding term linear in $\Delta\mu$ because $d_{wl}^{(1)}$ is a fixed quantity [see Eq. (2.30)]. However, let us mention that those complete wetting terms, which are nonlinear in $\Delta\mu$ and which have been omitted in Eq. (2.30), exhibit a similar feature as the aforementioned term in Eq. (3.13) concerning the dependence on the choice ν. Thus in the case of interfacial wetting this feature is more acute than in the one-component case. However, it is *without consequences* as far as the equilibrium thickness of the wetting film is concerned because these problematic terms drop out upon minimizing $\omega(l)$. For that reason we do not pursue this point further. We blame our poor choice of the trial functions off coexistence for this unwanted feature because they exhibit discontinuities [see Eqs. (2.28) and (3.12)] which become larger further away from coexistence. We expect this—in principle unwanted feature—to disappear for a more sophisticated choice of trial functions as far as complete wetting is concerned.

At the end of this subsection we want to discuss the physical implications of the results presented above. Our first observation is that the leading coefficient a_2 turns out to be the same as the one obtained within the sharp-kink approximation. This means that the transition temperature T_w for critical wetting, $a_2(T = T_w) = 0$, can be determined from the temperature dependence along the triple line of those six *bulk* densities, which characterize the three coexisting phases, and from the *leading* term of each interaction potential. In order to underscore this statement further, one could study in addition the influence of the extra tails as in Sec. II E. In face of the complexity of such calculations we refrained to do so in the case of binary liquid mixtures. However, since the one-component case must be included in the binary case [see the second paragraph after Eq. (3.19)] and since in the former case the incorporation of these extra tails did not change the coefficients a_2, a_3, and a_4 at all [see Eqs. (2.51)–(2.53)], we have no reason to suspect that in the binary case these extra tails would change the expressions in Eqs. (3.14)–(3.16). Thus, as in the one-component case we regard Eqs. (3.14)–(3.16) to be valid exactly. This lends additional reliability to the work performed in Ref. 14 whose analysis is based on the expression for a_2 as given in Eqs. (3.14) and (3.17).

In the one-component case T_w marks not only the wetting transition temperature for the wall-gas interface but also that temperature at which the wall-liquid interface structure undergoes a qualitative change [see Eq. (2.19)]. Thus the question arises whether the condition $a_2(T_w) = 0$ leads to a similar statement for the interface profiles in binary liquid systems. Indeed, the condition $\sum_{i,j} T_{ij,3} = 0$ leads to certain restrictions on weighted sums over i for the van der Waals amplitudes $A_{i,3}^{(\lambda;\kappa,\nu)}$. However, in contrast to the one-component case, the complicated formulas in Eq. (3.9) did not allow us to extract a simple interpretation of these restrictions.

As already stated above the value at $T = T_w$ of the coefficient $a_3(T)$ for the next-to-leading order term in the effective interface potential determines the order of the wetting transition. If $a_3(T_w) > 0$, critical wetting occurs, whereas there is first-order wetting if $a_3(T_w) < 0$.[1] In order to discuss our predictions for the order of interfacial wetting it is useful to compare them with the corresponding ones for the wetting of a wall in the particular case that all particles interact according to Lennard-Jones potentials and that the wall is a homogeneous medium. This means that $t_4 = u_4 = 0$ and $t_{ij,4} = 0$. In this case one obtains in the one-component system $a_3(T_w) = -\rho_l \Delta\rho t_3 d_{wl}^{(1)}$. By neglecting that contribution to $d_{wl}^{(1)}$, which stems from $z > \bar{z}_0$ [see Fig. 1(a)], Kroll and Meister[17] assumed that $d_{wl}^{(1)}$ is temperature independent and basically given by the sum of the atomic radii of the substrate and fluid atoms, respectively, and therefore it is a positive quantity. This would imply that $a_3(T_w) < 0$ and the wetting of a wall in Lennard-Jones systems would be always first order due to this *excluded volume effect* near the wall. However, as can be seen in Fig. 1(a), even for pure Lennard-Jones systems it is by no means obvious that $d_{wl}^{(1)}$ is always a positive quantity, so that even in this case critical wetting is conceivable. Furthermore, as emphasized in Ref. 8, for real substrates there are many correction terms to the leading behavior of the substrate potential (e.g., induced by the layered structure of the substrate) so that in general $u_4 \neq 0$. Thus for a Lennard-Jones fluid $a_3(T_w) = \Delta\rho(\frac{1}{3}\rho_w u_4 - \rho_l t_3 d_{wl}^{(1)})$. Consequently, the order of the wetting transition depends delicately on the external parameter u_4 introduced by the presence of the wall.

In Ref. 17 Kroll and Meister, without an explicit calculation, speculated also about the order of interfacial wet-

ting in binary liquid mixtures. They presented arguments that in a fluid system the effective pair interactions decay $\sim r^{-6}+O(r^{-8})$ for large separations r. This implies $t_{ij,4}=0$. Therefore one can argue that, in contrast to the case of wetting of a wall, where $u_4 \neq 0$, the corresponding quantities $t_{ij,4}$ in the binary liquid mixture are zero by reasons of symmetry and due to the fast rotations of the molecules.[17] Kroll and Meister continued their line of arguments by stating correctly that the absence of a hard wall in the case of interfacial wetting leads to the absence of the packing effects close to the wall—which are the ultimate reason for the nonzero excluded volume $d_{wl}^{(1)}$—because in this case all interfacial profiles are smooth and monotonic. Thus Kroll and Meister drew the reasonable conclusion that for interfacial wetting there is no excluded volume effect. Because they regarded this excluded volume as an obstacle for the occurrence of critical wetting [which is, however, according to our results not necessarily the case (see our remarks above)] their final conclusion was that critical wetting is more likely to occur in a binary liquid mixture than for the wetting of a wall.

We are now in the position to check this expectation against our explicit analytic results. For pure Lennard-Jones systems we have $a_3^{(0)}=0$ so that in this case

$$\hat{a}_3(T_w)=\delta_{\alpha\beta,1}(T_{BA,3}+T_{BB,3})-\delta_{\beta\gamma,1}(T_{AB,3}+T_{BB,3}) \; . \tag{3.33}$$

Note that *all* quantities on the right-hand side of Eq. (3.33) depend on temperature; here they are evaluated at $T=T_w$, which is defined implicitly by $\sum_{i,j} T_{ij,3}=0$. Therefore we arrive at the surprising result that the lengths $\delta_{\alpha\beta,1}$ and $\delta_{\beta\gamma,1}$ have the same meaning for interfacial wetting as the length $d_{wl}^{(1)}$ for wetting of a wall.

Based on the definitions for these lengths in Eqs. (3.29) we can therefore state the following conclusion: The differences between the zeroth moments of the A-density profile and the B-density profile of the free α-β and β-γ interface, respectively, play the same role as the excluded volume effect for wetting of a wall. This astonishing result contradicts the expectations of Kroll and Meister[17] and demonstrates the importance of describing interfacial wetting by two density profiles. In a one-density theory these lengths $\delta_{\alpha\beta,1}$ and $\delta_{\beta\gamma,1}$ would be zero and one would expect a multicritical wetting transition.

Of course one would now be interested in obtaining quantitative results for $\hat{a}_k(T_w)$ for specific systems in order to predict their corresponding order of the wetting transition. However, the lengths $\delta_{\alpha\beta,1}$ and $\delta_{\beta\gamma,1}$ are not accessible to analytic calculations. Therefore we postpone this necessarily numerical work to a future study. In any case our analysis shows the remarkable feature that both the *transition temperature* for critical interfacial wetting and the *separatrix* between first- and second-order wetting are determined completely by the *bulk* densities along the triple line, by the *leading* term of each interaction potential, and by certain zeroth moments of the emerging *free* interfaces.

Finally, as already stated in Sec. II D, close to T_c the effective interface potential for binary liquid mixtures exhibits the same features as the one for wetting of a wall; this becomes transparent by switching to the new variables $M(z)=\rho_A(z)-\rho_B(z)$ and $Q(z)=\rho_A(z)+\rho_B(z)$ (see Ref. 14). Therefore our discussion in Sec. II D, which is concerned with the effect of the vicinity of a critical point on wetting transitions, carries over to the present case if the interfacial wetting transition T_w happens to occur close to the critical end point $T_{\rm CEP}$. This is relevant for analyzing the experimental findings reported in Ref. 29; the corresponding discussion is presented in Sec. II D.

IV. SUMMARY

We have analytically studied wetting transitions of the wall-gas interface in a one-component fluid as well as interfacial wetting in binary liquid mixtures. We have paid particular attention to the consequences of the power-law decay of the intermolecular interactions and the resulting presence of van der Waals tails in the density profiles. *Inter alia* we have obtained the following results.

(1) We have reanalyzed the asymptotic behavior of the wall-liquid, liquid-gas, and wall-gas interface profiles in the one-component fluid (see Secs. II B and II C as well as Fig. 1). We have discussed their behavior and demonstrated the irrelevance of van der Waals tails close to criticality (end of Sec. II D). In addition, we have presented the corresponding formulas for the three possible fluid interface structures in binary liquid mixtures (Sec. III B).

(2) At a continuous wetting transition of a wall-gas interface, which takes place on the gas side of the coexistence curve, i.e., μ_0^-, also the wall-liquid interface on the liquid side μ_0^+ of the coexistence curve undergoes a qualitative change: below T_w the wall-liquid interface profile approaches its bulk value ρ_l from below and above T_w from above (Sec. II B and Fig. 2).

(3) The asymptotic behavior of the effective interface potential for large thicknesses l of the wetting film has been determined analytically by taking into account all aspects of the spatial variations of the density profiles [Secs. II D, II E, and III C, in particular Eqs. (2.29)–(2.35) and Eqs. (3.13)–(3.17)].

(4) We have explored the variety of possible definitions of effective interface potentials. We have shown that all of them lead to identical predictions for the intrinsic physical properties of the system under consideration (Appendix A and Sec. III C).

(5) The first three expansion coefficients of the effective interface potential can be expressed completely in terms of the leading behavior of the interaction potentials, the bulk densities, and certain moments of the emerging free interfaces. Consequently these data also determine the transition temperature for critical wetting and the separatrices between first-, second-, and third-order wetting transitions (Secs. II D, II E, and III C).

(6) The fourth term in the effective interface potential involves the logarithm of the thickness of the wetting film [Eqs. (2.30) and (3.13)].

(7) The distortion of the actual interface profiles containing a wetting film of finite thickness l compared with those following from a suitable superposition of the em-

erging free interfaces does not affect the first three terms of the effective interface potential (Sec. II E).

(8) In the one-component case the presence of the wall leads to an excluded volume effect, which—together with the first correction term to the leading behavior of the substrate potential—determines the order of the wetting transition. The excluded volume effect is determined by the zeroth moment of the wall-liquid interface profile and exhibits a pronounced temperature dependence, in particular close to T_c, due to the effect of critical adsorption. Its sign depends in integrated form on all details of the microscopic interaction potentials (Sec. II D).

(9) In the case of interfacial wetting in binary liquid mixtures the differences between the zeroth moments of an A-particle density profile and the B-particle density profile of the two emerging free interfaces, respectively, play the same role as the excluded volume effect for wetting a wall. Due to the absence of the first correction terms $\sim r^{-7}$ in the microscopic interactions in binary liquid mixtures, here this quasiexcluded volume effect has even stronger repercussions on the order of the wetting transition than in the case of wetting a wall (Sec. III C).

(10) Intrinsic moments of the free interface profiles enter into the expressions for all the terms in the effective interface potential [Eqs. (2.30) and (3.13)] with the exception of the Hamaker constant.

(11) The asymptotic power-law singularity for continuous wetting is confined to a critical temperature interval which is proportional to $T_c - T_w$. Therefore, if the wetting transition happens to occur close to T_c, the detection of its corresponding asymptotic thermal singularities becomes increasingly difficult. This prediction seems to check with recent experimental findings (Sec. II D and Fig. 4).

(12) Close to T_c the effects of critical adsorption and complete wetting compete. For $T \to T_c$ the power-law behavior $l \sim (\Delta\mu)^{-1/3}$ for complete wetting is confined to a rapidly decreasing wedge $\Delta\mu < \Delta\mu_c \sim (T_c - T)^{1.92}$, outside of which critical adsorption behavior with $l \sim (\Delta\mu)^{-0.402}$ prevails. This shows explicitly how the van der Waals interactions, which lead to the $(\Delta\mu)^{-1/3}$ law, become irrelevant upon approaching T_c compared with the critical phenomena, which lead to the more singular $(\Delta\mu)^{-0.402}$ law (Sec. II D and Fig. 4).

APPENDIX A: VARIOUS DEFINITIONS OF THE EFFECTIVE INTERFACE POTENTIAL

The results in Eqs. (2.30)–(2.37) can be rewritten in the following way:

$$\omega(l) = \hat{\omega}(\hat{l}) = (\mu_0 - \mu)(\Delta\rho\hat{l} - \rho_l d_{wl}^{(1)}) + \sum_{k=2}^{4} \hat{a}_k \hat{l}^{-k} + O(\hat{l}^{-5}\ln\hat{l}) , \tag{A1}$$

with $\hat{l} = l + d_{lg}^{(1)}$, $\hat{a}_2 = a_2$, $\hat{a}_3 = a_3^{(0)}$, and

$$\hat{a}_4 = a_4^{(0)} + 3a_2[d_{lg}^{(2)} - (d_{lg}^{(1)})^2] . \tag{A2}$$

$a_2, a_3^{(0)}, a_4^{(0)}$ are uniquely specified, because $d_{wl}^{(i)}$, $i = 1,2$, are defined unambiguously. However, according to our way of calculating $\omega(l)$ [see Eq. (2.26)], the values of $d_{lg}^{(i)}$ depend on the definition of what we denote as the thickness l of the wetting layer for a given density profile $\rho(z)$. Let us now consider two arbitrary definitions I and II with the corresponding values $l_{\rm I}$, $l_{\rm II}$, $d_{lg,\rm I}^{(i)}$, and $d_{lg,\rm II}^{(i)}$. As explained in Fig. 3 one has $l_{\rm II} = l_{\rm I} + \Delta z$. Correspondingly, $d_{lg,\rm I}^{(i)}$ is evaluated with $\rho_{lg,\rm I}(z)$ [see Eq. (2.37)] and $d_{lg,\rm II}^{(i)}$ with $\rho_{lg,\rm II}(z) = \rho_{lg,\rm I}(z + \Delta z)$; $\rho_\infty^{shk}(z)$ is the same for both. A shift of the integration variable leads to the following relations:

$$d_{lg,\rm II}^{(1)} = d_{lg,\rm I}^{(1)} - \Delta z \tag{A3}$$

and

$$d_{lg,\rm II}^{(2)} = d_{lg,\rm I}^{(2)} - 2\Delta z d_{lg,\rm I}^{(1)} + (\Delta z)^2 . \tag{A4}$$

Thus $\hat{l}_{\rm II} = l_{\rm II} + d_{lg,\rm II}^{(1)} = (l_{\rm I} + \Delta z) + (d_{lg,\rm I}^{(1)} - \Delta z) = \hat{l}_{\rm I}$ so that $\hat{l}$ is a thickness, which is independent of our definitions and thus a well-defined property of a given density profile $\rho(z)$. Due to Eqs. (A3) and (A4) the same is true for $d_{lg}^{(2)} - (d_{lg}^{(1)})^2$. Consequently, also $\hat{a}_4$ in Eq. (A2) is well specified and thus $\hat{\omega}(\hat{l})$ is independent from our choice of defining l.

One possible definition of (large) l is that it gives the distance between the wall and that point of the emerging liquid-gas interface within $\rho(z)$, which corresponds in the limit $l \to \infty$ to the position of the equimolar interface of the free liquid-gas interface. For that definition of l one has

$$d_{lg,e}^{(1)} = 0 . \tag{A5}$$

In this case we get ($\Delta\mu = \mu_0 - \mu$, e stands for equimolar)

$$\omega_e(l_e) = \Delta\mu(\Delta\rho l_e - \rho_l d_{wl}^{(1)}) + \frac{a_2}{l_e^2} + \frac{a_3^{(0)}}{l_e^3} + \frac{a_4^{(0)} + 3a_2 d_{lg,e}^{(2)}}{l_e^4} + O(l_e^{-5}\ln l_e) . \tag{A6}$$

At this point we want to emphasize that for $k \geq 4$ the coefficients $A_k^{(\gamma)}$ in Eq. (2.23) depend on the definition of the center of the free interface profile. In accordance with our above notation one has $A_{3,\rm II}^{(\gamma)} = A_{3,\rm I}^{(\gamma)}$,

$$A_{4,\rm II}^{(\gamma)} = A_{4,\rm I}^{(\gamma)} \pm 3A_{3,\rm I}^{(\gamma)}\Delta z , \tag{A7}$$

and

$$A_{5,\rm II}^{(\gamma)} = A_{5,\rm I}^{(\gamma)} \pm 4A_{4,\rm I}^{(\gamma)}\Delta z + 6A_{3,\rm I}^{(\gamma)}(\Delta z)^2 , \tag{A8}$$

where the upper sign is valid for $\gamma = l$ and the lower sign for $\gamma = g$. Thus we obtain as invariant coefficients $\hat{A}_3^{(\gamma)} = A_3^{(\gamma)}$,

$$\hat{A}_4^{(\gamma)} = A_4^{(\gamma)} \pm 3A_3^{(\gamma)} d_{lg}^{(1)} , \tag{A9}$$

and

$$\hat{A}_5^{(\gamma)} = A_5^{(\gamma)} \pm 4A_4^{(\gamma)} d_{lg}^{(1)} + 6A_3^{(\gamma)}(d_{lg}^{(1)})^2 . \tag{A10}$$

In the next step we determine the coverage Γ for the density profiles described by Eqs. (2.26) and (2.28). One obtains

$$\Gamma = (l + d_{lg}^{(1)})\Delta\rho - \rho_l d_{wl}^{(1)} + I_1 + I_2 + I_3 \tag{A11}$$

with

$$I_1=-\int_{\kappa(l)-\lambda(l)}^{\infty}dz\,[\rho_{wl}(z)-\rho_l]\ , \tag{A12}$$

$$I_2=\int_{-\lambda(l)}^{\lambda(l)}dz\,[G(z)-\rho_l]\ , \tag{A13}$$

and

$$I_3=\int_{-\infty}^{-l+\kappa(l)+\lambda(l)}dz\,[\rho_{lg}(z)-\rho_l]\ . \tag{A14}$$

Equations (A12)–(A14) show that the coverage Γ is invariant in the above sense [i.e., it is the same for $\rho_{\rm I}(z,l)$ and $\rho_{\rm II}(z,l+\Delta z)$, which are identical profiles] if and only if $\kappa(l)=\hat{\kappa}(\hat{l})$ and $\lambda(l)=\hat{\lambda}(\hat{l})$, i.e., if these functions are taken to depend only on the invariant thickness $\hat{l}=l+d_{lg}^{(1)}$ and on invariant combinations of $d_{lg}^{(1)}$. If in our trial function we take $\hat{\lambda}(\hat{l}\to\infty)\sim\hat{l}^{-(1+\epsilon)}$, $\epsilon>0$, as mentioned in the main text, one has $I_2=O(\hat{l}^{-4-\epsilon})$. With $\hat{\kappa}(\hat{l})=\kappa_0\hat{l}[1+\kappa_1\hat{l}^{-1}+\kappa_2\hat{l}^{-2}+O(\hat{l}^{-3})]$ one finally obtains from Eqs. (A11)–(A14)

$$\bar{l}\equiv\frac{\Gamma}{\Delta\rho}=\hat{l}+\gamma_0+\sum_{k=2}^{4}\gamma_k\hat{l}^{-k}+\cdots\ , \tag{A15}$$

with

$$\gamma_0=-\frac{\rho_l}{\Delta\rho}d_{wl}^{(1)}\ , \tag{A16}$$

$$\gamma_2=-\frac{1}{2\Delta\rho}[Q_3^{(l)}\kappa_0^{-2}-\hat{A}_3^{(l)}(1-\kappa_0)^{-2}]\ , \tag{A17}$$

$$\gamma_3=-\frac{1}{3\Delta\rho}[Q_4^{(l)}\kappa_0^{-3}-3Q_3^{(l)}\kappa_1\kappa_0^{-2}-\hat{A}_4^{(l)}(1-\kappa_0)^{-3}-3\hat{A}_3^{(l)}\kappa_0\kappa_1(1-\kappa_0)^{-3}]\ , \tag{A18}$$

and

$$\gamma_4=-\frac{1}{4\Delta\rho}[Q_5^{(l)}\kappa_0^{-4}-4Q_3^{(l)}\kappa_2\kappa_0^{-2}+6Q_3^{(l)}\kappa_1^2\kappa_0^{-2}-4Q_4^{(l)}\kappa_1\kappa_0^{-3}-\hat{A}_5^{(l)}(1-\kappa_0)^{-4}-4\hat{A}_3^{(l)}\kappa_0\kappa_2(1-\kappa_0)^{-3}-6\hat{A}_3^{(l)}\kappa_0^2\kappa_1^2(1-\kappa_0)^{-4}-4\hat{A}_4^{(l)}\kappa_0\kappa_1(1-\kappa_0)^{-4}]\ . \tag{A19}$$

By using Eqs. (A1), (A2), and (A15)–(A19) we are finally able to express the effective interface potential in terms of the coverage $\Gamma=\bar{l}\Delta\rho$:

$$\omega(l)=\bar{\omega}(\bar{l})=\Delta\mu\Delta\rho\bar{l}+\sum_{k=2}^{4}\bar{a}_k\bar{l}^{-k}+\cdots\ , \tag{A20}$$

with

$$\bar{a}_2=\hat{a}_2-\Delta\mu\Delta\rho\gamma_2\ , \tag{A21}$$

$$\bar{a}_3=\hat{a}_3+2\gamma_0\hat{a}_2-\Delta\mu\Delta\rho(\gamma_3+2\gamma_0\gamma_2)\ , \tag{A22}$$

and

$$\bar{a}_4=\hat{a}_4+3\gamma_0\hat{a}_3+3\gamma_0^2\hat{a}_2-\Delta\mu\Delta\rho(\gamma_4+3\gamma_3\gamma_0+3\gamma_2\gamma_0^2)\ . \tag{A23}$$

Equations (A15)–(A23) show explicitly that $\bar{\omega}(\bar{l})$ is invariant, i.e., it is independent of any definition of l from which we started to obtain $\bar{\omega}(\bar{l})$. It is interesting to compare $\hat{\omega}(\hat{l})$ and $\bar{\omega}(\bar{l})$. The corresponding former expansion coefficients $\hat{a}_k$, $k=2,3,4$ [see Eq. (A2)], are determined uniquely by the characteristics of the wall-liquid and the liquid-gas interface profiles alone. At coexistence ($\Delta\mu=0$) the same is true for the expansion coefficients $\bar{a}_k$. However, off coexistence these coefficients depend, in addition, on the matching position for the wall-liquid and liquid-gas interface profiles in order to form a smooth trial function. (γ_2, γ_3, and γ_4 depend on κ_0, κ_1, and κ_2 and so do $\bar{a}_2$, $\bar{a}_3$, and $\bar{a}_4$ for $\Delta\mu>0$.) These dependences should not be confused with the problem of having various options for defining l. This reflects the fact that the coverage Γ does depend on this matching position [see Eq. (A15)]. However, even off coexistence the detail of matching, i.e., the function $G(z)$ [see Eq. (2.26)], does not influence the first four leading terms of the effective interface potential (see Appendix B).

In order to make our reasoning transparent let us summarize the results of Appendix A. Generally speaking, the effective interface potential $\omega(l)+\sigma_{wl}+\sigma_{lg}$ is the minimum of $\Omega[\{\rho(z)\}]$ under the restriction that $\rho(z)$ exhibits a wetting film with a prescribed thickness l. For l there are several possible definitions, which we denote by μ. One can, e.g., require that $\Omega[\{\rho(z)\}]$ is minimized under the restriction that $\rho(z=l)=(\rho_l+\rho_g)/2$ or that $\rho''(z=l)=0$, etc. This leads to various $\omega_\mu(l)$, which differ from each other. If they have been determined exactly, all those properties which follow from the unrestricted minimum of $\Omega[\{\rho(z)\}]$ (like T_w, the location of separatrices, the minimum value itself, etc.) must be reproduced by *any* $\omega_\mu(l)$, i.e., independent of μ.

We calculate $\omega_\mu(l)$ approximately according to Eq. (2.26), which means that for any of the aforementioned possible definitions of l we have to find the corresponding point z_μ^* on the free liquid-gas interface and with that we then enter into Eq. (2.26). If we have two definitions of l, μ and ν, which for a given profile differ by $\Delta z(l)$, $l_\mu=l_\nu-\Delta z(l)$, one must have quite generally $\omega_\nu(l)=\omega_\mu(l-\Delta z(l))$, because a given density profile renders a well-defined value of $\Omega[\{\rho(z)\}]$ irrespective of what thickness l we assign to it. Because $\Delta z(l)$ is not known in advance, the various effective interface potentials cannot easily be translated into each other. [In general, the distance between those points where $\rho''(z)=0$ and $\rho(z)=(\rho_g+\rho_l)/2$, respectively, depends on l.] According to our special way of calculating $\omega(l)$ we obtain various $z_\mu^*=z_\nu^*-\Delta z$ and with them $d_{lg,\mu}^{(1)}=d_{lg,\nu}^{(1)}+\Delta z$. Here, Δz does not depend on l. Combining this with the general result above we arrive at $\omega_\nu(l)=\omega_\mu(l+d_{lg,\nu}^{(1)}-d_{lg}^{(1)})$ so that $\omega_\nu(l+d_{lg,\mu}^{(1)})=\omega_\mu(l+d_{lg,\nu}^{(1)})$. Furthermore, due to Eq. (A1) we find that $\omega_\nu(l)=\hat{\omega}(l+d_{lg,\nu}^{(1)})$ where the function $\hat{\omega}$ is *independent* of ν. Thus our explicit results do satisfy the equation in the last but one sen-

tence, which must hold on general grounds. In face of the enormous length of the analytic calculations and the complexity of the expressions involved this represents a highly nontrivial consistency check.

Thus we find within our approximate expressions for the various definitions of the effective interface potential $\omega_\mu(l)=\hat{\omega}(l+d_{lg,\mu}^{(1)})$ that they are all parametrized by a single length $d_{lg,\mu}^{(1)}$. Since they differ only by a shift of l one can easily translate them into each other. Furthermore, this implies that all the properties of the minima of $\omega_\mu(l)$ are the same for all μ. Thus all intrinsic properties of the system (T_w, separatrices, etc.) are also independent of μ. This can also be checked directly on the basis of Eqs. (2.30)–(2.35). Since the coverage Γ is independent from any definition of l we expect that if we derive the effective interface potential as a function of Γ from our expression for $\omega_\mu(l)$ the dependence on μ must drop out. According to Eqs. (A20)–(A23) this is indeed the case. $\bar{\omega}(l)$ is equally suited as an effective interface potential as $\omega_\mu(l)$; in $\bar{\omega}$ one has an integral restriction on $\rho(z)$, whereas in ω_μ one has various local ones at $z=l$. $\bar{\omega}(l)$ clearly differs from $\omega_\mu(l)$ but again as it must be they predict the same intrinsic properties of the system. This can be checked on the basis of Eqs. (A20)–A(23).

APPENDIX B: RELEVANCE OF THE MATCHING CONDITIONS

According to Eq. (2.26) the trial function $\rho(z,l;T)$ matches smoothly the wall-liquid interface profile and the liquid-gas interface profile. The transition region $\kappa(l)-\lambda(l)\le z\le\kappa(l)+\lambda(l)$ induces a contribution $\delta\omega$ to the effective interface potential. With $\kappa(l\to\infty)=\kappa_0 l+\cdots$ it has the form

$$\delta\omega(l)=\delta_1+\delta_2 l^{-2}+\delta_3 l^{-3}+\delta_4 l^{-4}+\cdots , \tag{B1}$$

where

$$\delta_1=\int_{-\lambda}^{\lambda}dz\,[f_h(G(z,l),T)-f_h(\rho_l,T)]-(\mu-w_0\rho_l)\int_{-\lambda}^{\lambda}dz\,[G(z,l)-\rho_l]$$
$$+\tfrac{1}{2}\int_{-\lambda}^{\lambda}dz\int_{-\lambda}^{\lambda}dz'\,\hat{w}(|z-z'|)[G(z,l)-\rho_l][G(z',l)-\rho_l] , \tag{B2}$$

$$\delta_2=0 , \tag{B3}$$

$$\delta_3=\int_{-\lambda}^{\lambda}dz\,[G(z,l)-\rho_l][(\rho_l t_3-\rho_w u_3)\kappa_0^{-3}+\Delta\rho t_3(1-\kappa_0)^{-3}+\kappa_0^{-3}Q_3^{(l)}t(\lambda-z)-(1-\kappa_0)^{-3}A_3^{(l)}t(\lambda+z)] , \tag{B4}$$

and

$$\delta_4=\int_{-\lambda}^{\lambda}dz\,[G(z,l)-\rho_l]\left[\sum_{i=1}^{8}\delta_{4,i}(z)\right] , \tag{B5}$$

with

$$\delta_{4,1}(z)=\kappa_0^{-4}[\rho_l t_4-\rho_w u_4+3(\rho_l t_3-\rho_w u_3)z] , \tag{B6}$$

$$\delta_{4,2}(z)=(1-\kappa_0)^{-4}\Delta\rho(t_4-3t_3 z) , \tag{B7}$$

$$\delta_{4,3}(z)=3\kappa_0^{-4}\rho_l^2 d_{wl}^{(1)}t_3 , \tag{B8}$$

$$\delta_{4,4}(z)=-3(1-\kappa_0)^{-4}\rho_l\Delta\rho d_{lg}^{(1)}t_3 , \tag{B9}$$

$$\delta_{4,5}(z)=\kappa_0^{-4}(Q_4^{(l)}+3\lambda Q_3^{(l)})t(\lambda-z) , \tag{B10}$$

$$\delta_{4,6}(z)=-(1-\kappa_0)^{-4}(A_4^{(l)}+3\lambda A_3^{(l)})t(\lambda+z) , \tag{B11}$$

$$\delta_{4,7}(z)=3\kappa_0^{-4}Q_3^{(l)}\int_{\lambda-z}^{\infty}dz't(z') , \tag{B12}$$

and

$$\delta_{4,8}(z)=-3(1-\kappa_0)^{-4}A_3^{(l)}\int_{\lambda+z}^{\infty}dz't(z') . \tag{B13}$$

The continuity of $\rho(z,l)$ and the presence of the van der Waals tail in $\rho_{wl}(z)$ and of that on the liquid side of $\rho_{lg}(z)$ (see Fig. 3) require the following asymptotic l dependence of $G(z,l)$ for large l and for any fixed value $\lambda=\bar{\lambda}$:

$$\max_{|z|\le\bar{\lambda}}(|G(z,l)-\rho_l|)\sim l^{-3} . \tag{B14}$$

Therefore one finds for large l

$$\left|\int_{-\lambda(l)}^{\lambda(l)}dz\,[G(z,l)-\rho_l]\right|\sim\lambda(l)l^{-3} . \tag{B15}$$

Along the same line of arguments it is straightforward to check that if $\lambda(l\to\infty)\sim l^{-(1+\epsilon)}$ one has $\delta\omega(l\to\infty)\sim l^{-4-\epsilon}$. Thus for any $\epsilon>0$, a_2, a_3, and a_4 do not depend on the details of matching the wall-liquid and the liquid-gas interface profile.

[1] S. Dietrich, in *Phase Transitions and Critical Phenomena*, edited by C. Domb and J. L. Lebowitz (Academic, London, 1988), Vol. 12, p. 1.

[2] D. E. Sullivan and M. M. Telo da Gama, in *Fluid Interfacial Phenomena*, edited by C. A. Croxton (Wiley, New York, 1986), p. 45.

[3] M. Schick, in *Liquids at Interfaces*, Les Houches Summer School Lectures, Session XLVIII, edited by J. Charvolin, J. F. Joanny, and J. Zinn-Justin (Elsevier, Amsterdam, 1990).

[4] E. Brézin, B. I. Halperin, and S. Leibler, J. Phys. (Paris) **44**, 775 (1983).

[5] T. Aukrust and E. H. Hauge, Phys. Rev. Lett. **54**, 1814 (1985).

[6] S. Dietrich and M. Schick, Phys. Rev. B **31**, 4718 (1985).

[7] C. Ebner, W. F. Saam, and A. K. Sen, Phys. Rev. B **31**, 6134 (1985).

[8] S. Dietrich and M. Schick, Phys. Rev. B **33**, 4952 (1986).

[9] M. Napiórkowski and S. Dietrich, Phys. Rev. B **34**, 6469 (1986).

[10]M. Napiórkowski and S. Dietrich, Europhys. Lett. **9**, 361 (1989).
[11]R. Evans, Adv. Phys. **28**, 143 (1979).
[12]S. Dietrich, M. P. Nightingale, and M. Schick, Phys. Rev. B **32**, 3182 (1985).
[13]J. H. Sikkenk, J. O. Indekeu, J. M. J. van Leeuwen, E. O. Vossnack, and A. F. Bakker, J. Stat. Phys. **52**, 23 (1988).
[14]S. Dietrich and A. Latz, Phys. Rev. B **40**, 9204 (1989).
[15]J. Barker and D. Henderson, Rev. Mod. Phys. **48**, 587 (1976).
[16]W. E. Carlos and M. W. Cole, Surf. Sci. **91**, 339 (1980), and references therein.
[17]D. M. Kroll and T. F. Meister, Phys. Rev. B **31**, 392 (1985).
[18]J. K. Percus and G. J. Yevick, Phys. Rev. **110**, 1 (1958).
[19]N. F. Carnahan and K. E. Starling, J. Chem. Phys. **51**, 635 (1969).
[20]A. Trayanov and E. Tosatti, Phys. Rev. Lett. **59**, 2207 (1987).
[21]B. C. Freasier and S. Nordholm, Mol. Phys. **54**, 33 (1985).
[22]T. F. Meister and D. M. Kroll, Phys. Rev. A **31**, 4055 (1985).
[23]W. A. Curtin and N. W. Ashcroft, Phys. Rev. Lett. **56**, 2775 (1986).
[24]J. A. Støvneng, T. Aukrust, and E. H. Hauge, Physica A **143**, 40 (1987).
[25]P. Pfeuty and G. Toulouse, *Introduction to the Renormalization Group and Critical Phenomena* (Wiley, Chichester, 1977), Secs. 2.3 and 2.4.
[26]H. W. Diehl, in *Phase Transitions and Critical Phenomena*, edited by C. Domb and J. L. Lebowitz (Academic, London, 1986), Vol. 10, p. 75.
[27]C. Ebner, W. F. Saam, and A. K. Sen, Phys. Rev. B **32**, 1558 (1985).
[28]J. S. Rowlinson and B. Widom, *Molecular Theory of Capillarity* (Clarendon, Oxford, 1982).
[29]L. M. Trejo, J. Gracia, C. Varea, and A. Robledo, Europhys. Lett. **7**, 537 (1988).
[30]In Ref. 10 $d_{lg}^{(1)}$ and $d_{lg}^{(2)}$ are denoted by d_0 and $2d_1$, respectively.
[31]In Ref. 10 $\hat{l}_0$ and $\hat{\tau}_c$ are denoted by $\hat{L}_0$ and $\hat{L}_0/\hat{L}_1$, respectively.
[32]This observation agrees with results from lowest-order low-temperature expansions [see Eqs. (13) and (17) in Ref. 17 and Ref. 26 in Ref. 27], which were not pursued there in further detail. We study these effects systematically and in particular close to T_c, which is out of reach for the first term of a low-temperature expansion.
[33]In general, one can have $D_k(l\to\infty)\sim l^{k-3}$. In this case, however, the check of the requirements (i)–(iii) becomes mathematically subtle: the absence of homogeneous convergence does not longer allow one to interchange the limit $l\to\infty$ with the infinite sum over k in Eq. (2.48). In addition, in this general case *all* coefficients D_k would generate contributions to a_k^*, $k\geq 3$. This would be prohibitive for any analytical analysis. Therefore we restrict ourselves to a trial function, in which not only D_3 but also all higher coefficients D_k are independent of l.
[34]R. F. Kayser, M. R. Moldover, and J. W. Schmidt, J. Chem. Soc., Faraday Trans. II **82**, 1701 (1986).
[35]Note that there is a misprint in Eq. (3.11) in Ref. 9. It should read $a_4=a_4^{(0)}+\frac{1}{4}(\chi_1^2+\chi_2^2)a_2^{(0)}$.